Advances in description of low-energy fission

Alexander Andreev

February, 2024

Joint Institute for Nuclear Research

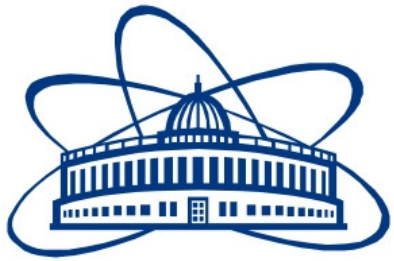

Outline

Spontaneous nuclear decay modes

Main characteristics of nuclear fission

Models for nuclear fission:

- Liquid-drop model
- Microscopic-macroscopic model
- Statistical scission-point model
- Dynamical calculations based on SPM

Spontaneous nuclear decay modes

Spontaneous nuclear decay modes

1. β-decay

- β^--decay:
  ${}^A_Z\mathrm{X} \rightarrow {}^A_{Z+1}\mathrm{Y} + e^- + \tilde{\nu}$
  $M(Z,A) > M(Z+1,A) + m_e$
  $(n \rightarrow p + e^- + \tilde{\nu})$

- β^+-decay:
  ${}^A_Z\mathrm{X} \rightarrow {}^A_{Z-1}\mathrm{Y} + e^+ + \nu$
  $M(Z,A) > M(Z-1,A) + m_e$
  $(p \rightarrow n + e^+ + \nu)$

- e-capture:
  ${}^A_Z X + e^- \rightarrow {}^A_{Z-1}\mathrm{Y} + \nu$
  $M(Z,A) > M(Z-1,A) + m_e$
  $(p + e^- \rightarrow n + \nu)$

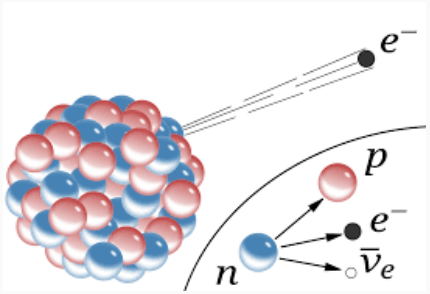

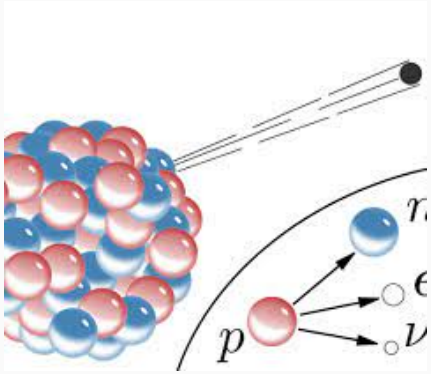

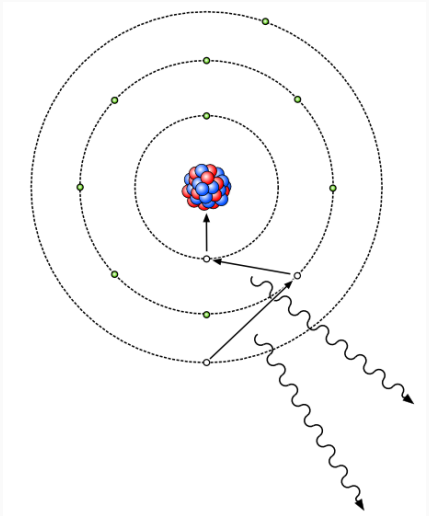

Spontaneous nuclear decay modes

2. α-decay ($Z > 83$)

   $^{A}_{Z}\mathrm{X} \rightarrow ^{A-4}_{Z-2}\mathrm{Y} + ^{4}_{2}\mathrm{He}$

   $M(Z, A) > M(Z-2, A-2) + M(^{4}_{2}\mathrm{He})$

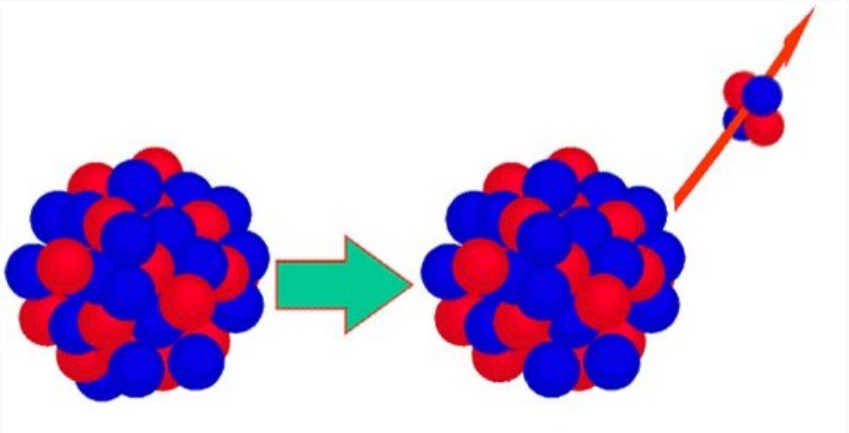

3. Proton or neutron emission

Nuclear fission: **Process of division of a nucleus into two or more fragments of comparable masses**

4. Fission ($Z \geq 90$)

$$^{A}_{Z}\mathrm{X} \rightarrow {}^{A_1}_{Z_1}\mathrm{Y}_1 + {}^{A_2}_{Z_2}\mathrm{Y}_2$$

$$A_1 + A_2 = A$$
$$Z_1 + Z_2 = Z$$

$$M(Z, A) > M(Z_1, A_1) + M(Z_2, A_2)$$

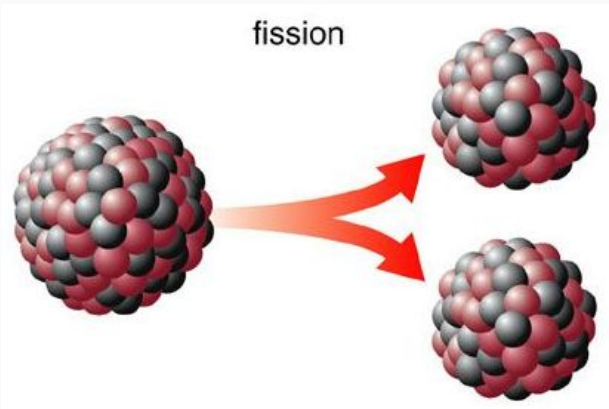

Nuclear chart

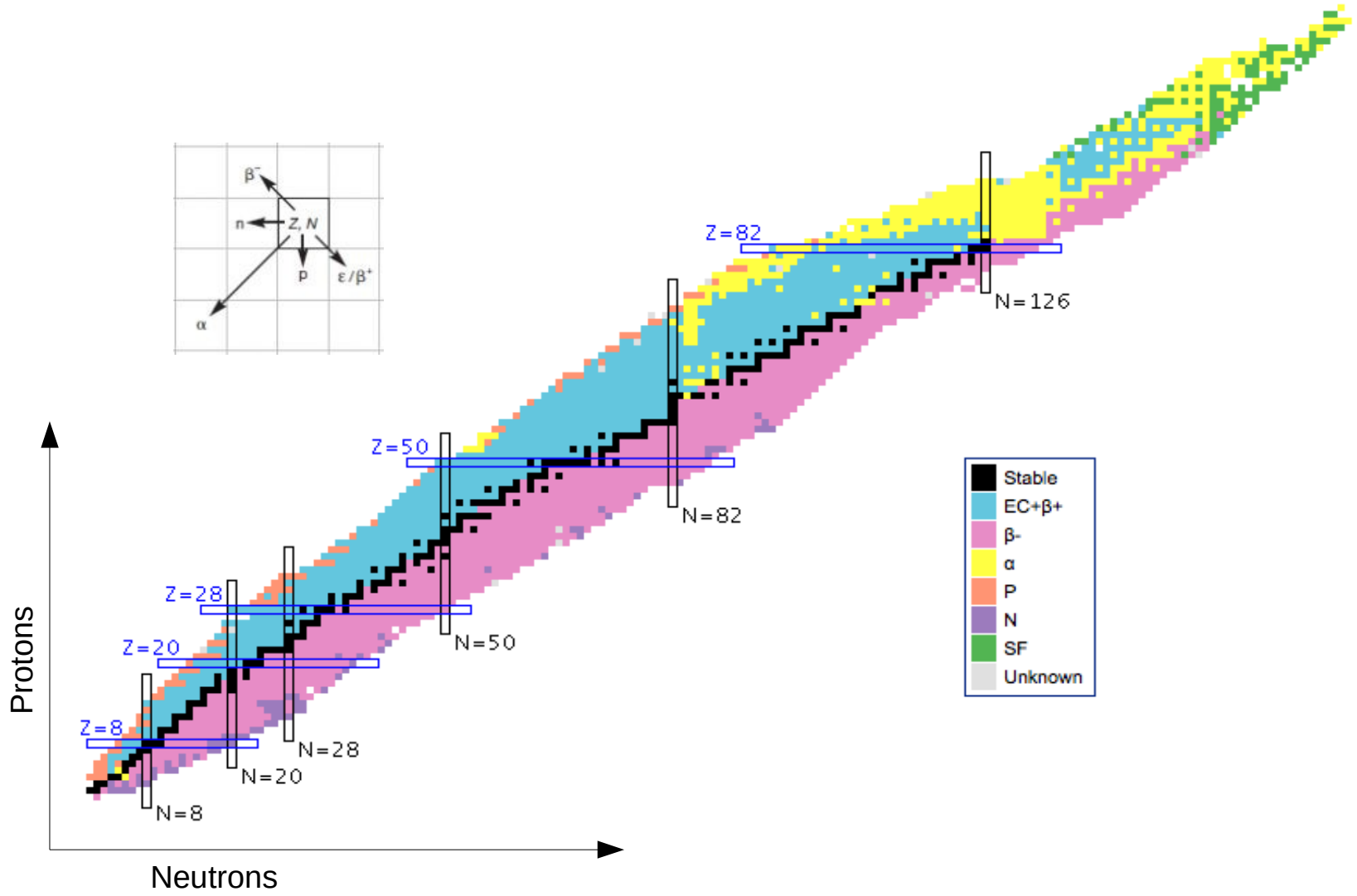

History

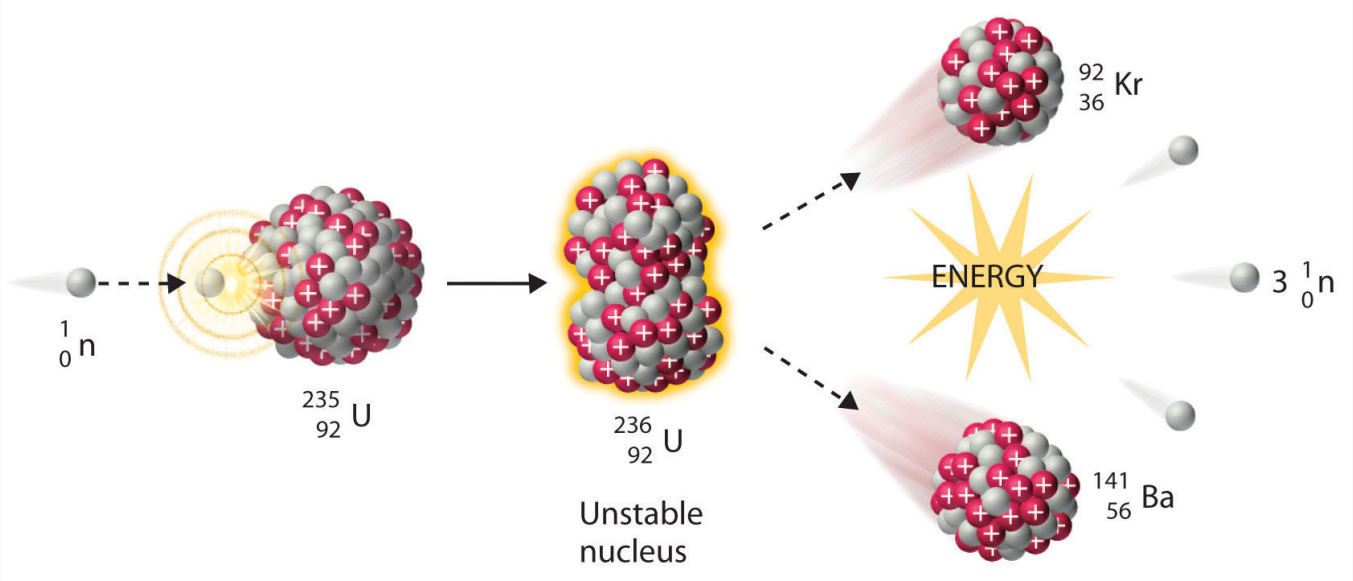

1938- Discovery of fission by Otto Hahn, Fritz Strassman, Lisa Meitner: Irradiation of Uranium resulted in products such as Ba and La

1940- G. N. Flerov reported that ^{238}U undergoes fission spontaneously

Fission types: $\begin{cases} \text{Spontaneous} - (Z \geq 90) \\ \text{Induced (Fission of excited nucleus)} \end{cases}$

Main characteristics of nuclear fission

Asymmetric fission mode

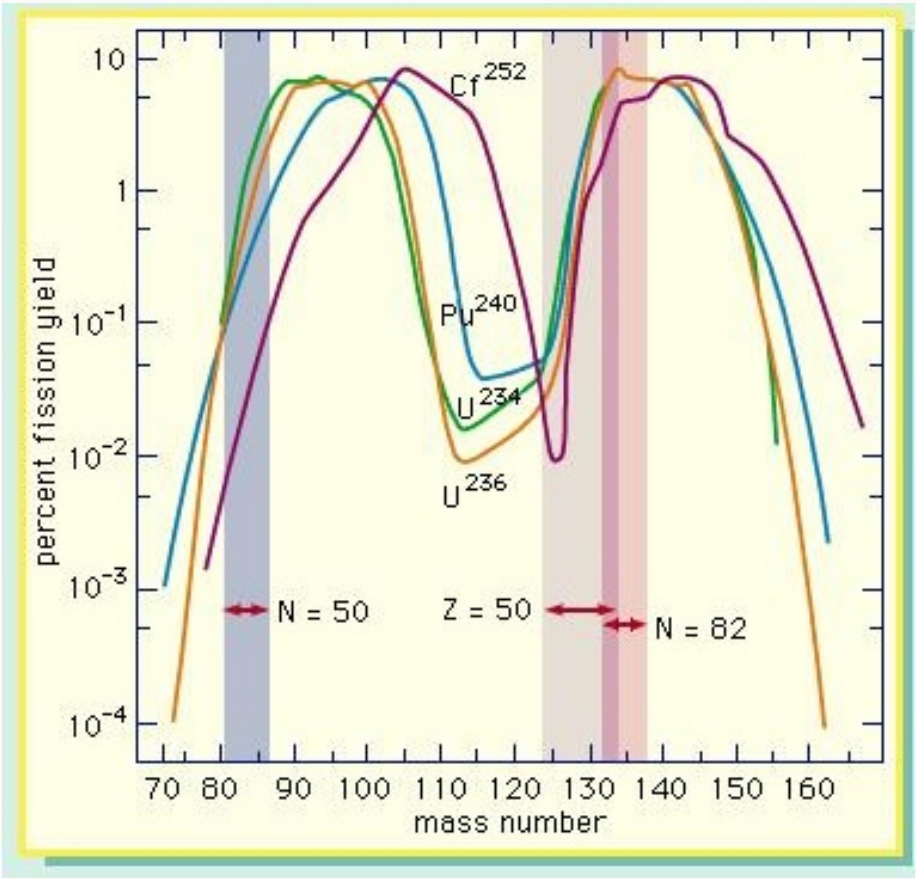

The light mass group shifts to higher masses as the mass of fissioning nucleus increases, while the heavy group remains nearly stationary. The shaded areas show the location of closed shells of 50 protons, 50 neutrons, and 82 neutrons.

Excitation dependence of mass distribution

At still higher energies, the curve becomes single-humped with a maximum yield for symmetric mass splits.

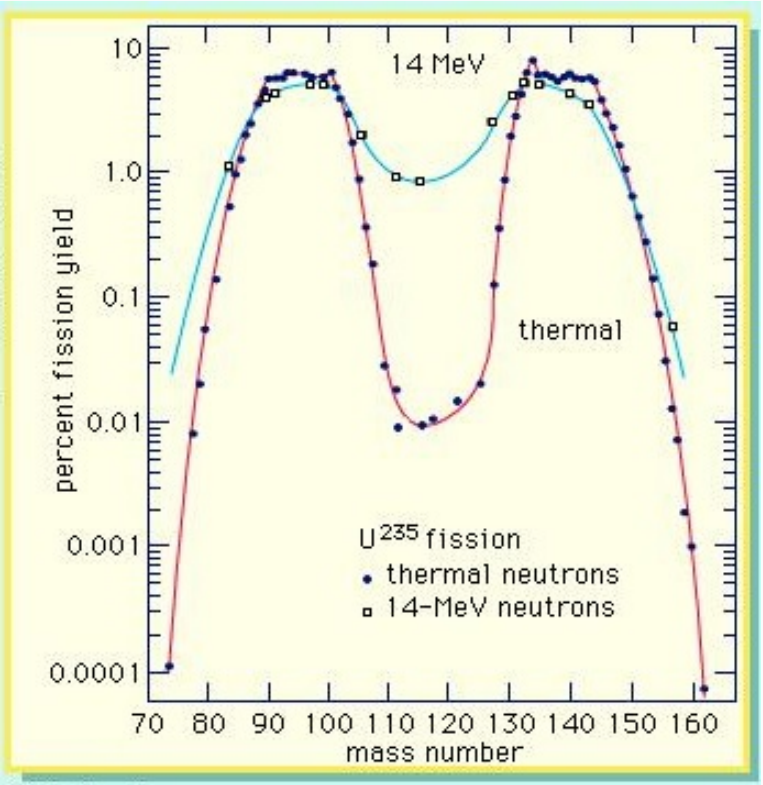

1) Mass and charge distributions

Symmetric fission mode

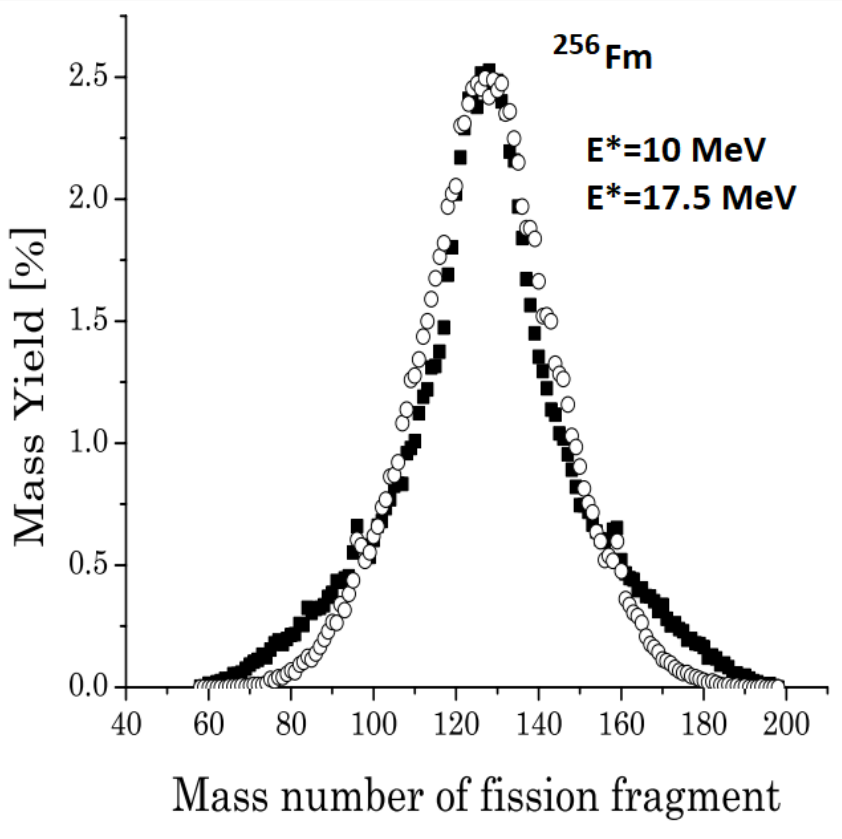

Coexistence of symmetric and asymmetric modes:

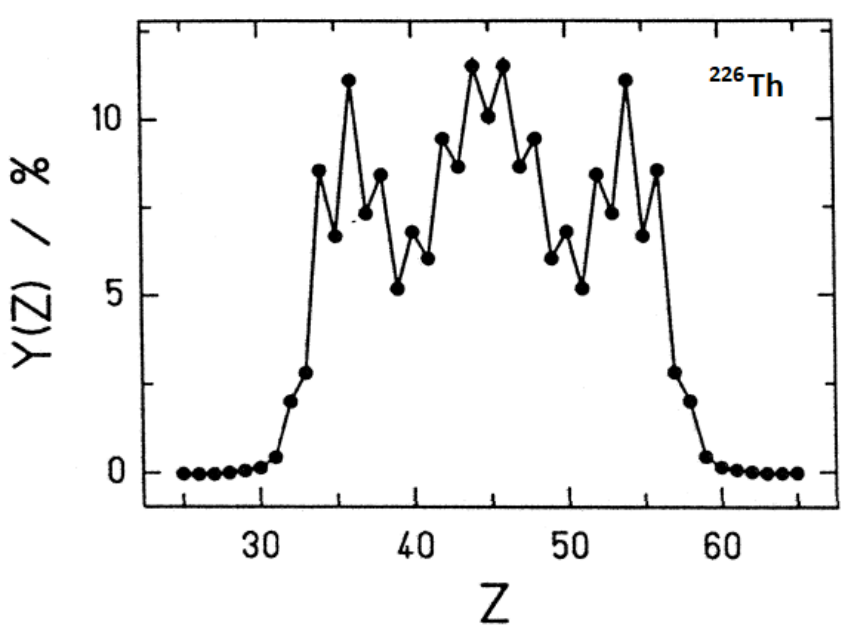

1) Mass and charge distributions

Transition between symmetric and asymmetric fission modes

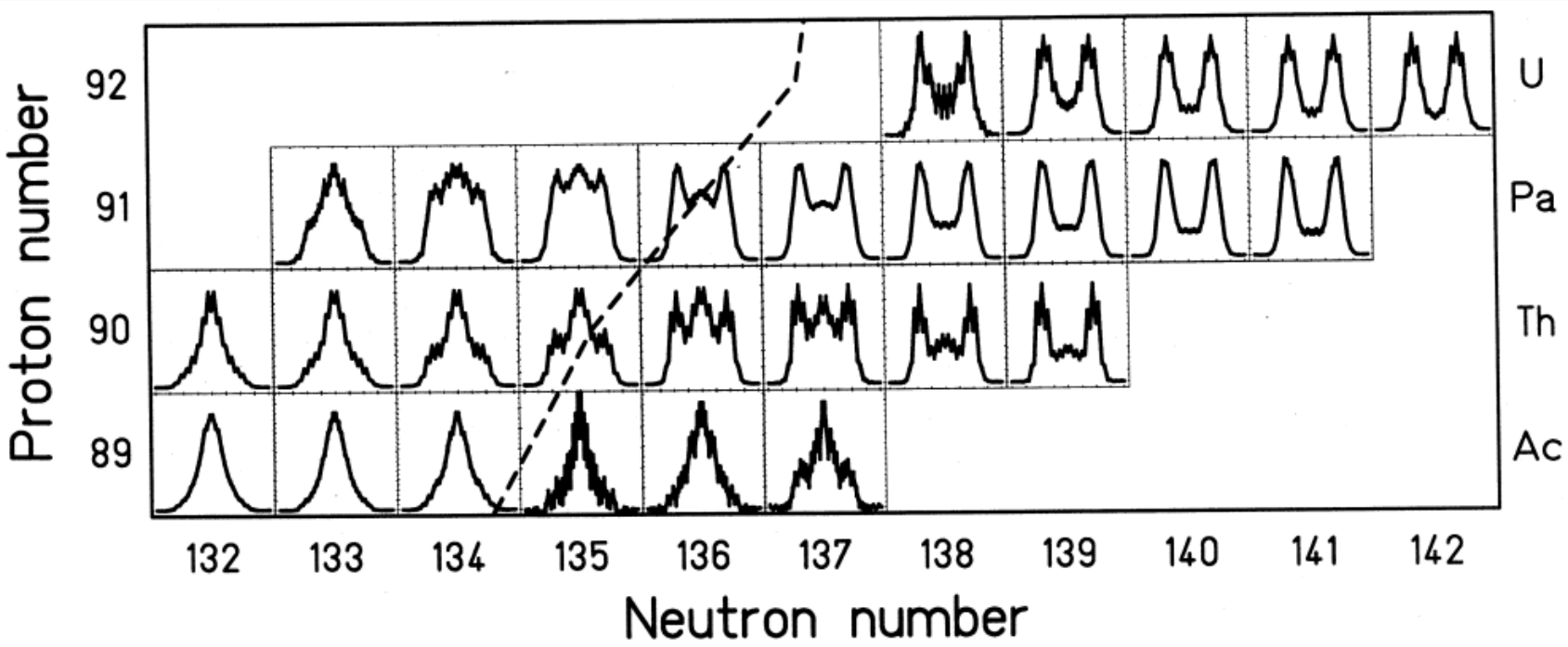

2) Kinetic energy of fission fragments

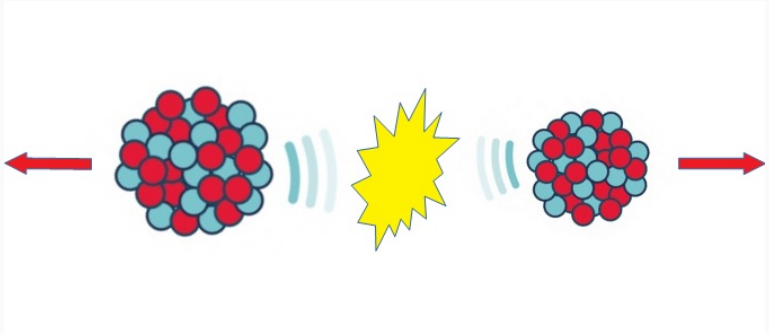

Conservation of momentum

$$m_L v_L = m_H v_H \rightarrow \frac{v_L}{v_H} = \frac{m_L}{m_H}$$

$$\frac{E_L}{E_H} = \frac{1/2 m_L v_L^2}{1/2 m_H v_H^2} = \frac{m_H}{m_L}$$

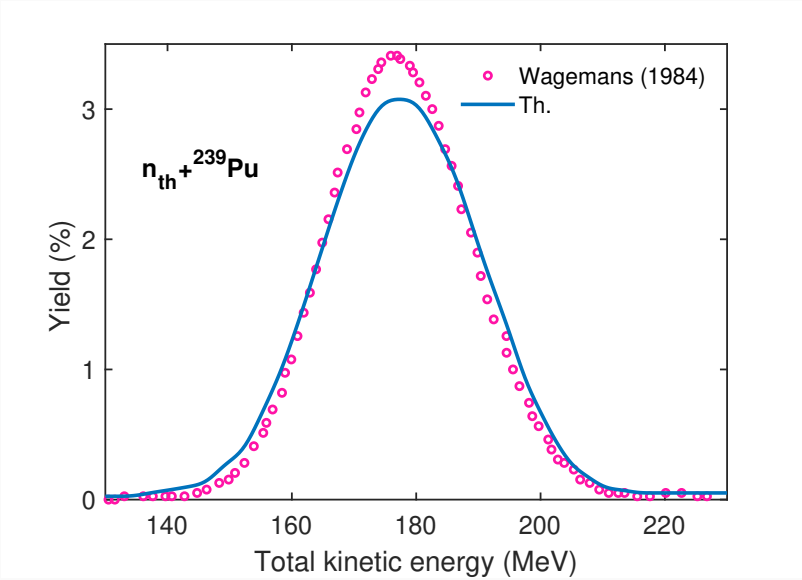

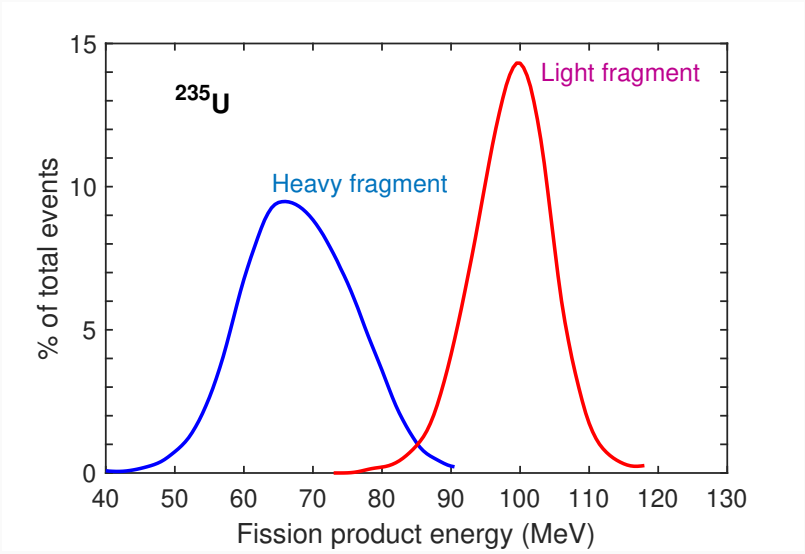

3) Neutron multiplicity: Number of emitted neutrons

Excitation of fission fragments leads to neutron emission after fission

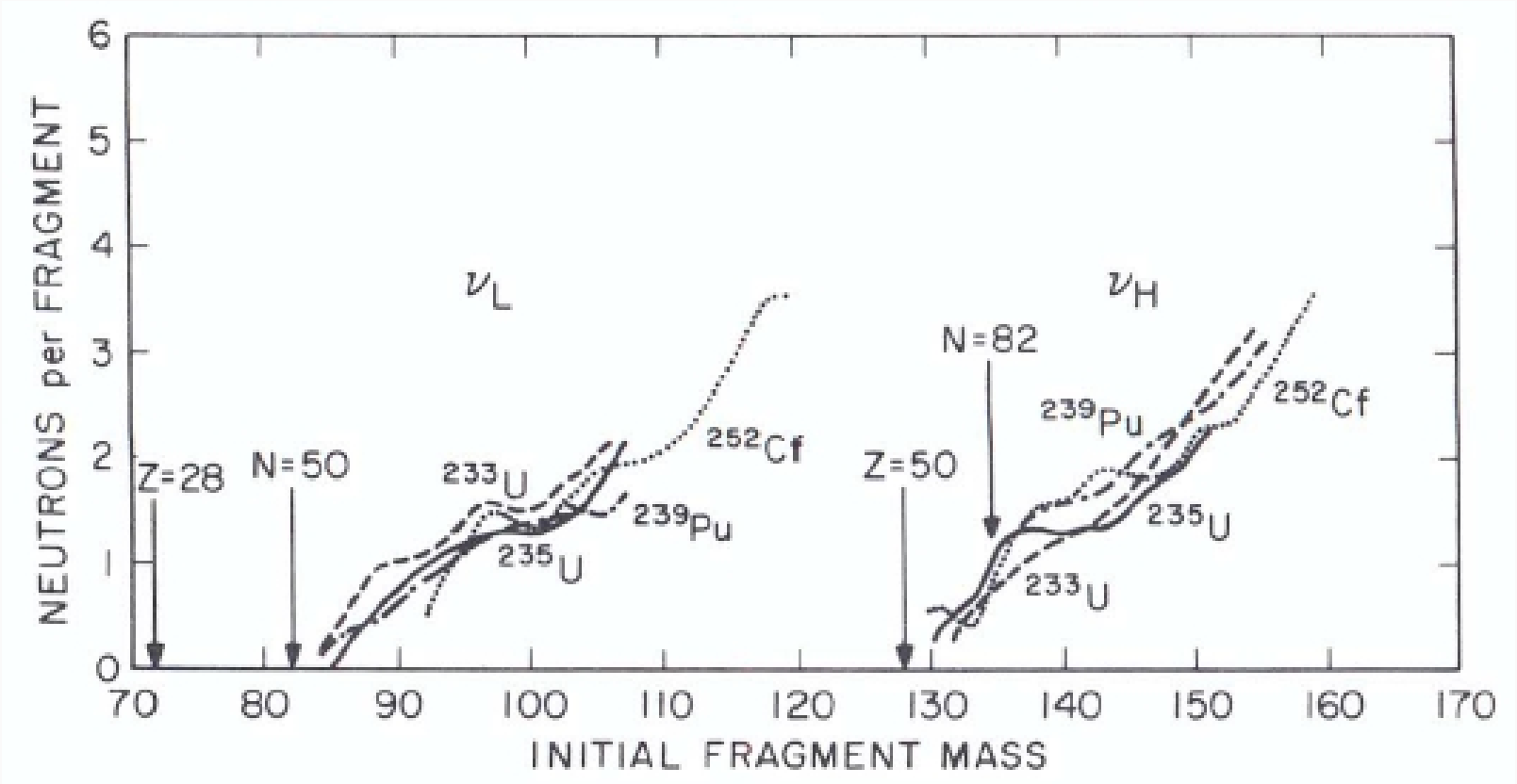

4) Spontaneous fission half-life

Nucleus	$T_{1/2}$ (SF), Years	$T_{1/2}$, Years	Branching ratio (%)
^{235}U	$(1.0 \pm 0.3)10^{17}$	$(7.04 \pm 0.01)10^{8}$	7×10^{-9}
^{238}U	$(8.2 \pm 0.1)10^{15}$	$(4.468 \pm 0.003)10^{9}$	5.5×10^{-5}
^{239}Pu	$(8 \pm 2)10^{15}$	$(2.411 \pm 0.003)10^{4}$	3×10^{-10}
^{240}Pu	$(1.151 \pm 0.04)10^{9}$	$(6.564 \pm 0.0011)10^{3}$	5.7×10^{-6}
^{246}Cm	$(1.82 \pm 0.02)10^{7}$	4760±40	2.62×10^{-2}
^{252}Cf	86 ± 1	2.645±0.008	3.09
^{254}Cf	60.7 days ±0.2	60.5 days ±0.2	99.7

Models for nuclear fission:

Why still fission?!

Despite all the understanding of the fission process, still no theory or model is able to predict all the fission observable in a consistent way for all possible fissioning systems in a wide energy range.

Problems:

- Too many nucleons for exact description of motion of each nucleon.
- Too few nucleons for using many-body methods.
- The exact nucleon-nucleon interaction is unknown.

No unified model for description of nucleus and nuclear reactions.

Different models for different mass regions, different effects, etc.

Fission process

For $A > 90$: $M(Z, A) > M(Z_1, A_1) + M(Z_2, A_2)$

But no fission for intermediate mass nuclei because of the fission barrier

Spontaneous fission : $Z \geq 90 \quad (A \sim 230)$

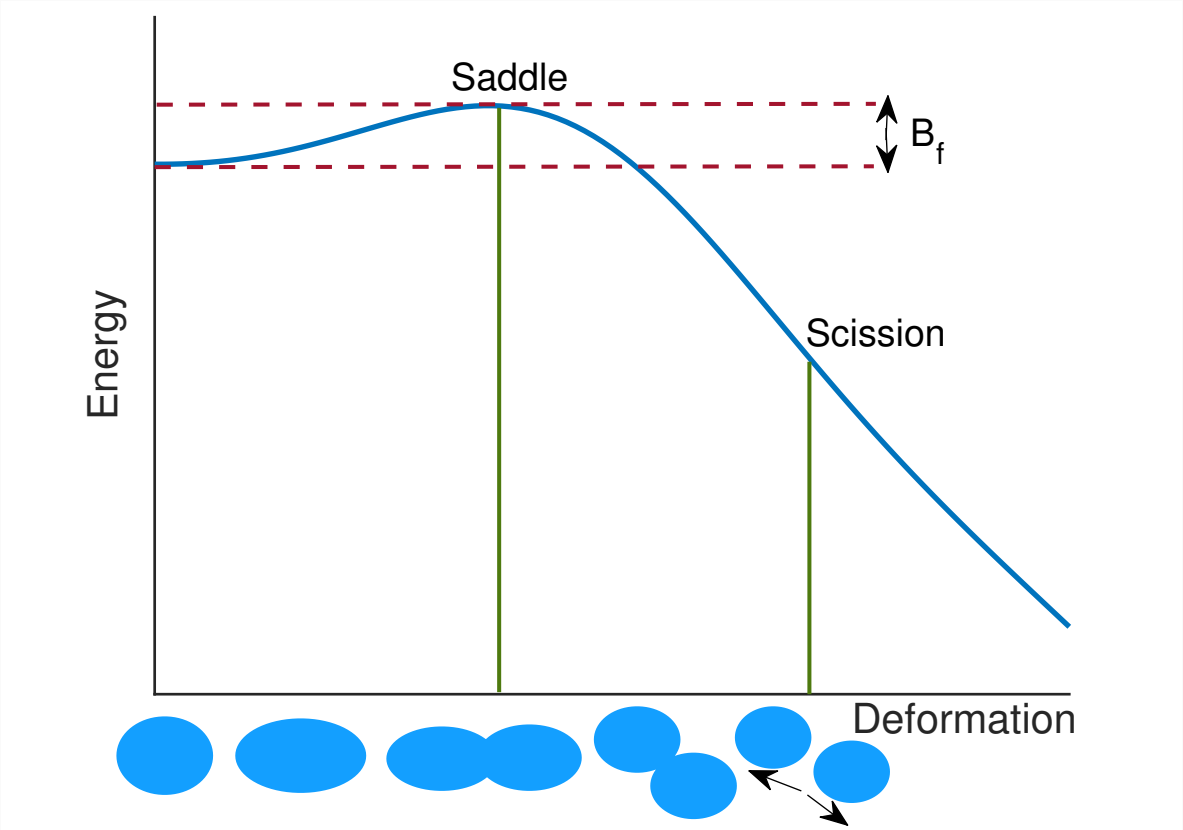

Shape parametrization

$$R = c_{vol} R_0 \left[1 + \sum_{\lambda,\nu} \alpha_{\lambda,\nu} Y_{\lambda,\nu}(\theta, \phi)\right]$$
$$\lambda = 2, 3, 4, \ldots \quad \nu = -\lambda, \ldots, +\lambda$$

c_{vol}- volume conservation parameter

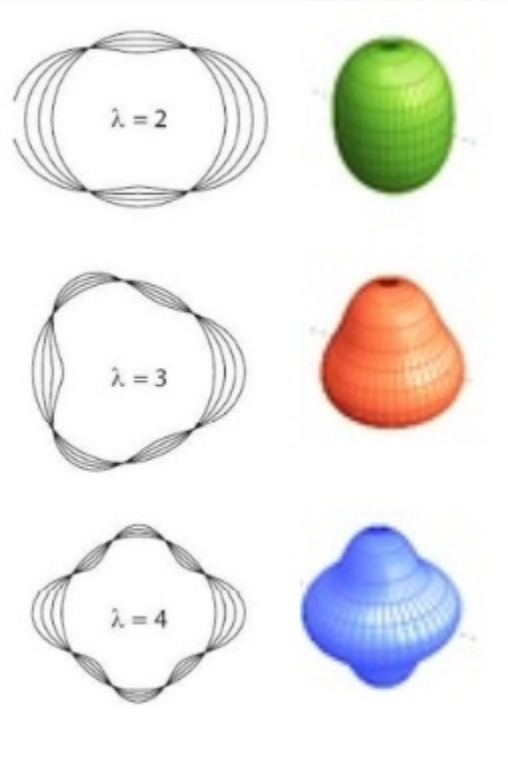

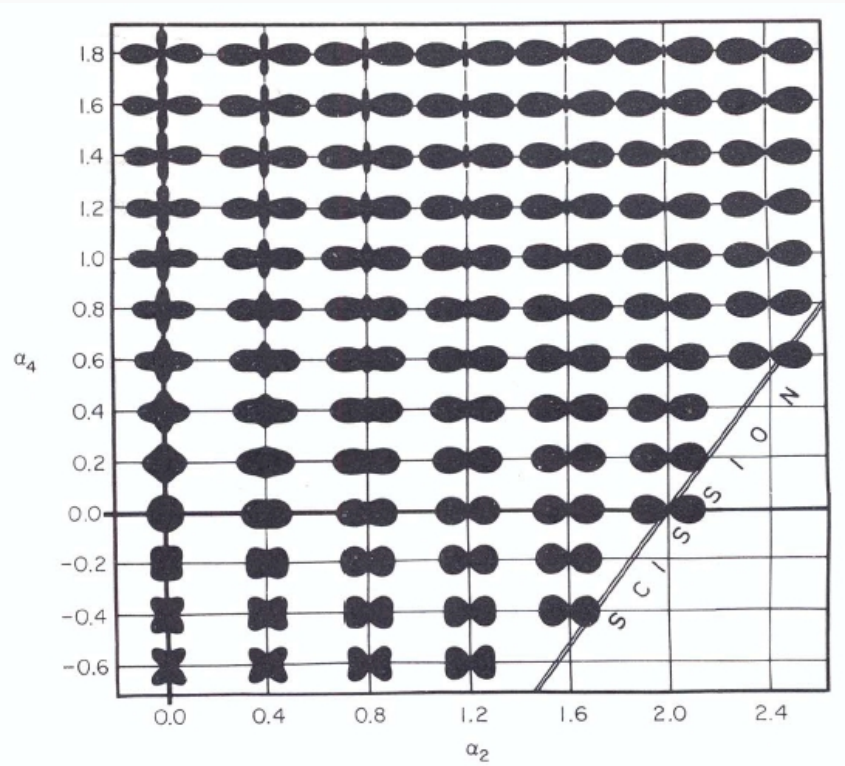

Main collective coordinates

- Elongation (Quadrupole deformation, β, β_2, α_{20}, etc.)

- Asymmetry (Octupole deformation, β_3, α_{30}, etc.)

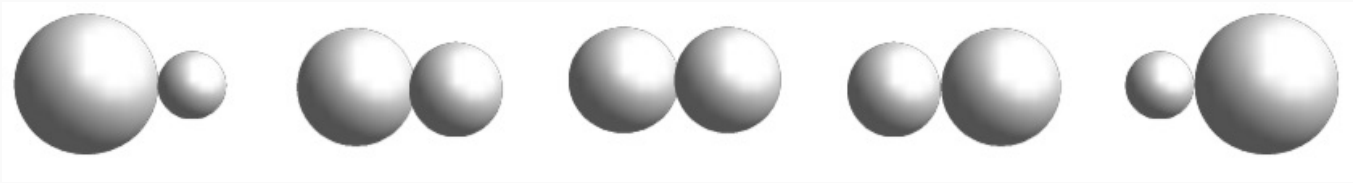

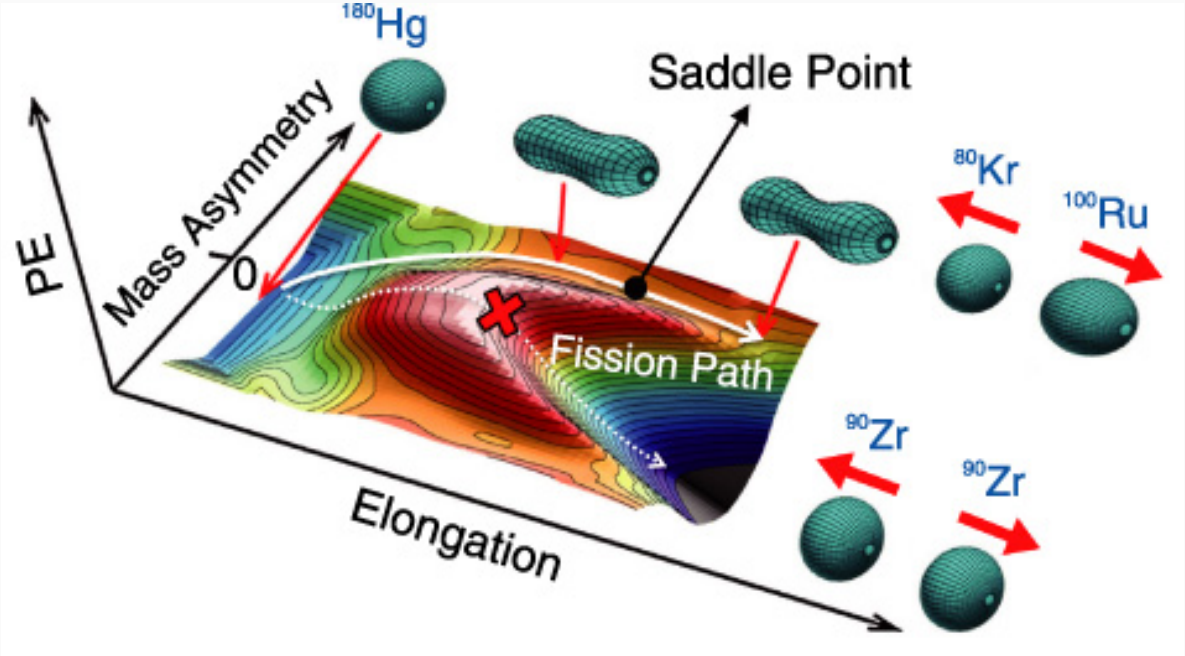

Study of fission process

- Parametrization of nuclear shape
- Calculation of potential energy surface as a function of deformations
- Determination of fission path, fission barrier

Liquid-drop model

Liquid-drop model

Nucleus is a drop of charged liquid:

- Incompressible
- No shell effects
- Uniform charge density

$$B(Z,N) = a_v A - a_s A^{2/3} - a_c \frac{Z^2}{A^{1/3}} - a_{symm} \frac{(Z-A/2)^2}{A} + \frac{\delta}{A^{1/2}}$$

$$\Downarrow$$

$$B(Z,N,\beta) = E_v - E_s(\beta) - E_c(\beta) - E_{symm}$$

Stability of the liquid drop

For small quadrupole deformations α_{20}:

$|\Delta E_c| < \Delta E_s$ -Drop is stable against small deformation

$|\Delta E_c| > \Delta E_s$ -Drop is unstable against small deformation

$$E_s = E_s^0 \left(1 + \frac{2}{5}\alpha_{20}^2\right)$$

$$E_c = E_c^0 \left(1 - \frac{1}{5}\alpha_{20}^2\right)$$

Fissility parameter:

$$x = \frac{|\Delta E_c|}{\Delta E_s} = \frac{E_c^0}{2E_s^0} = \frac{a_c \frac{Z^2}{A^{1/3}}}{2a_s A^{2/3}} = \frac{a_c}{2a_s}\frac{Z^2}{A}$$

$$\approx \frac{1}{50.13}\frac{Z^2}{A}$$

$x < 1$ -stable, $x > 1$ -unstable

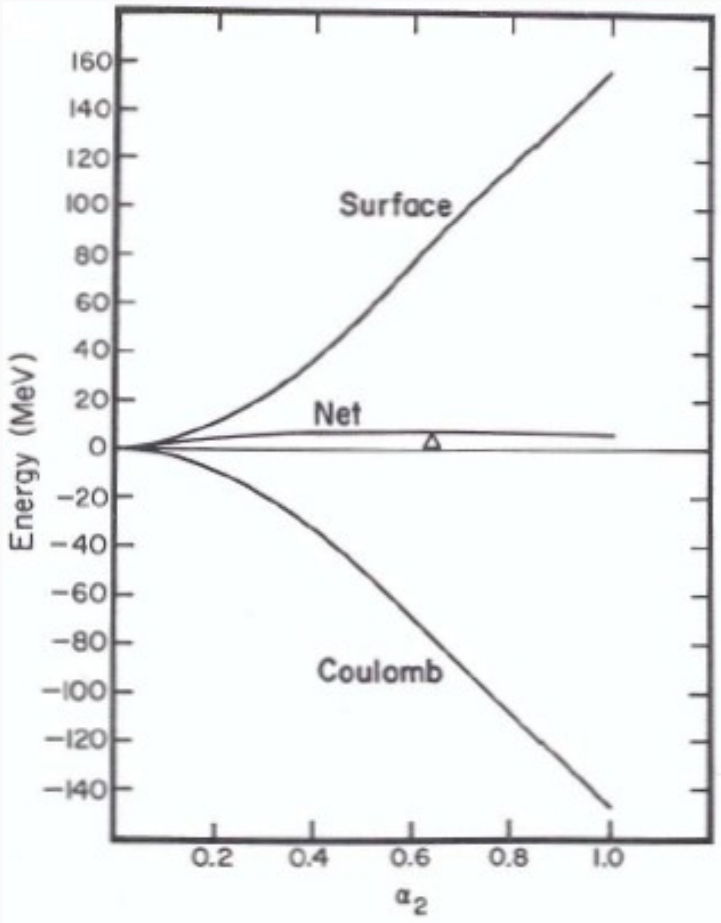

Fission barrier height - Fissility parameter

$$x = \frac{1}{50.13}\frac{Z^2}{A}$$

^{238}U:

$Z^2/A = 35.56$

$x = 0.71$

^{252}Cf:

$Z^2/A = 38.11$

$x = 0.76$

Liquid-drop model calculations

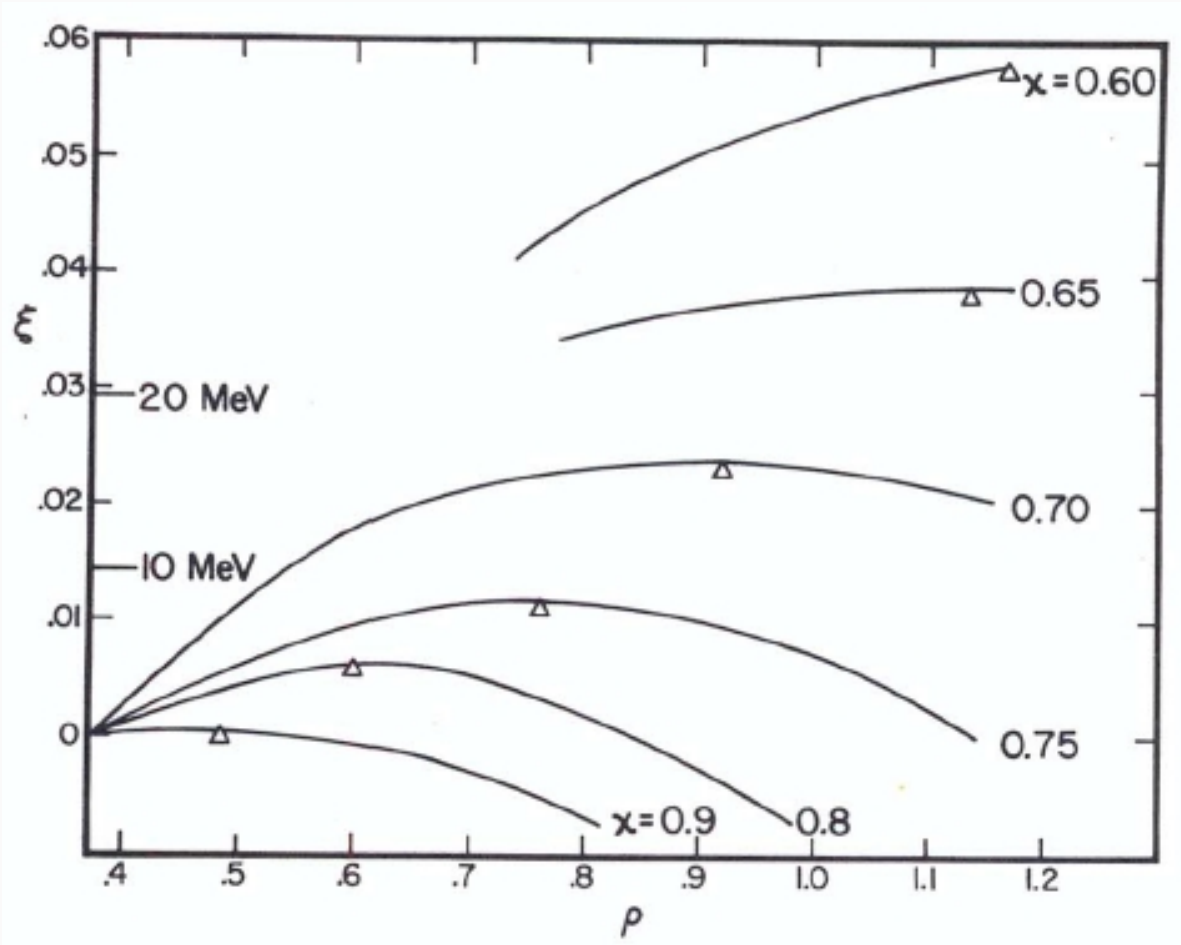

$\xi = \frac{E}{E_s^0}$

Fission barrier height

Comparison with experiment

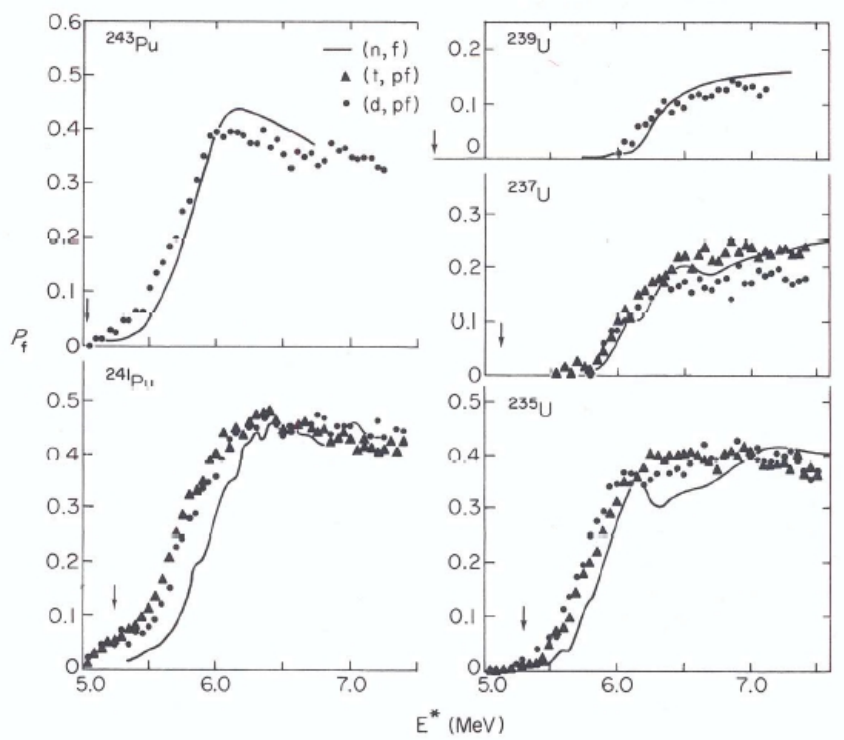

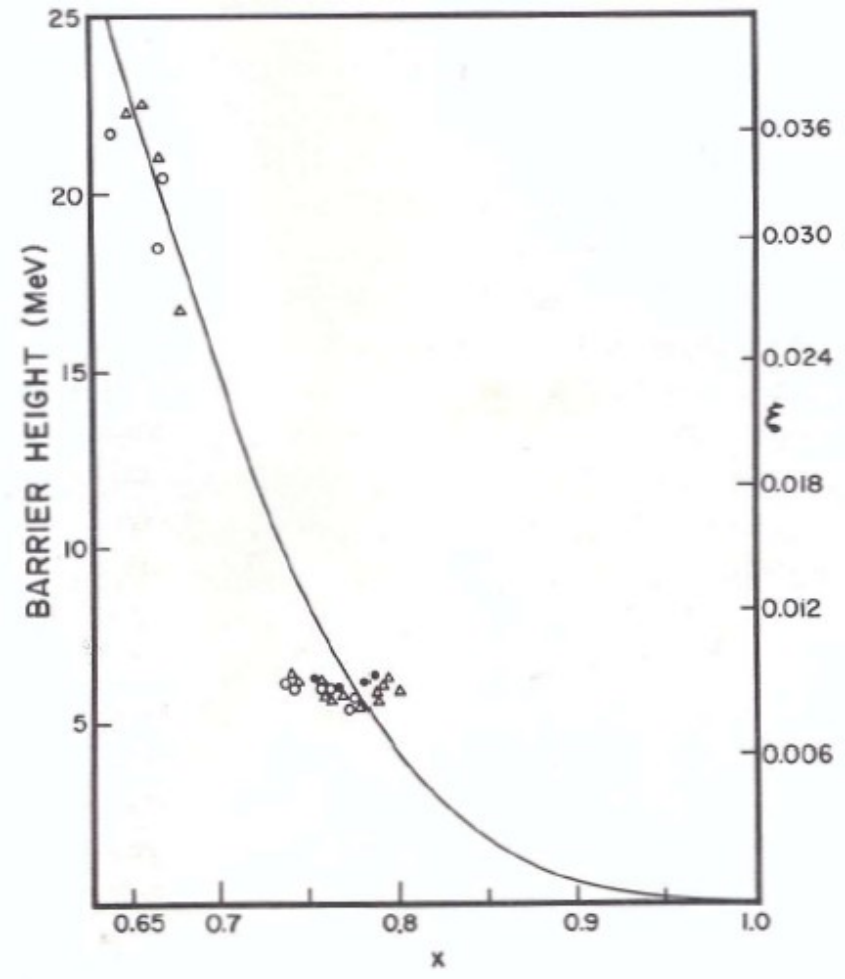

Asymmetric fission with liquid drop model

No asymmetric fission in liquid-drop model!

Search for stable asymmetric deformation (asymmetric minimum of the energy):

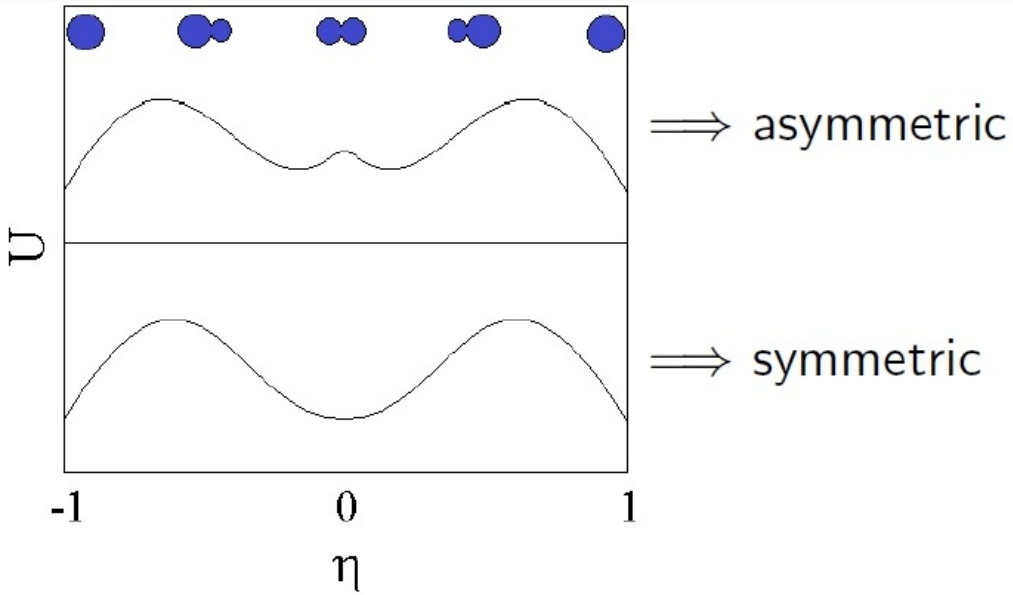

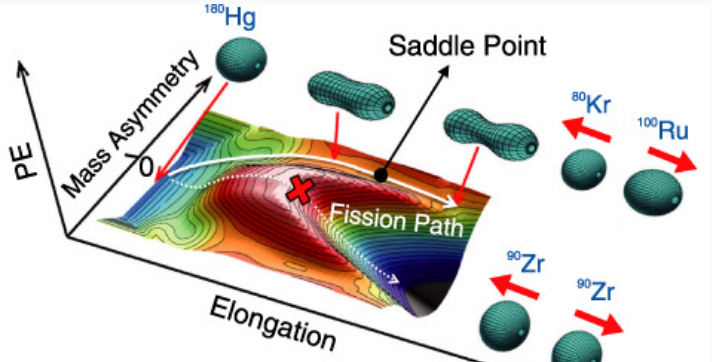

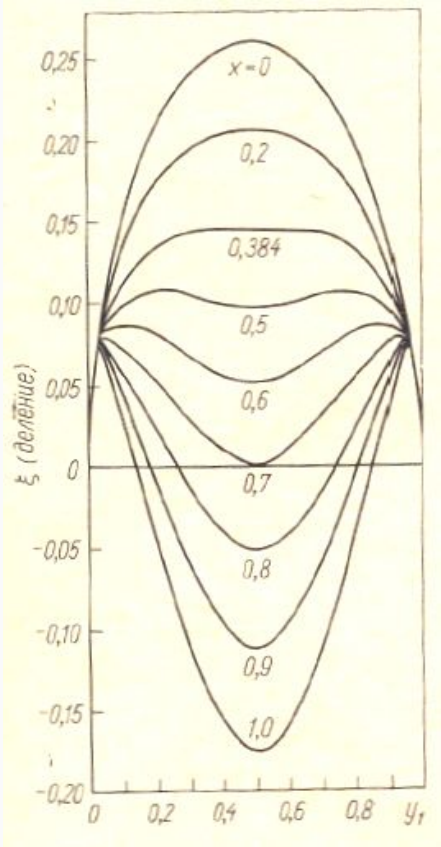

Potential energy at the scission point as a function of asymmetry ($y_1 = A_1/A$)

Microscopic-macroscopic model

Microscopic-Macroscopic model

Failure of pure microscopic shell model: rise of energy at large deformations

$$E(\beta) = \sum_{i(occupied)} E_i(\beta) + Coulomb$$

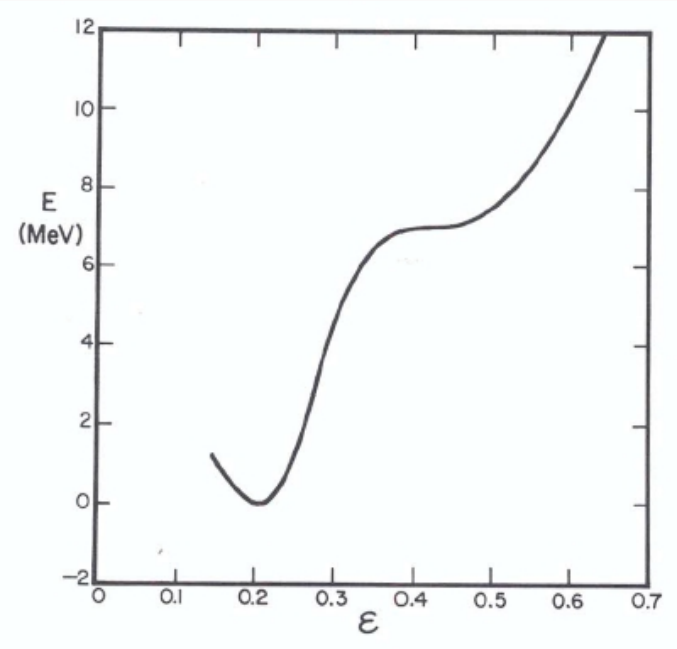

Shell correction method of Strutinsky

1. Subtraction of shell deviations from smoothed energy curve of pure shell model.
2. Adding these deviations to macroscopic energy of liquid-drop model.

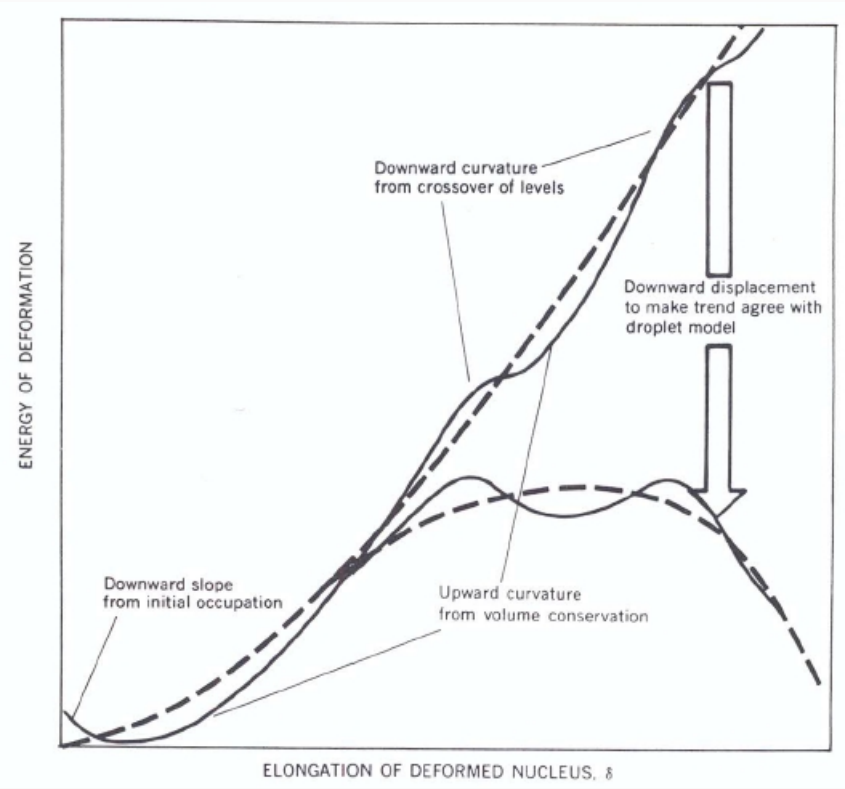

Shell corrections E_{shell}

Adding to binding energy due to irregularities of single-particle spectrum. (V. M. Strutinsky, Nucl. Phys. A, 95, 420, 1967)

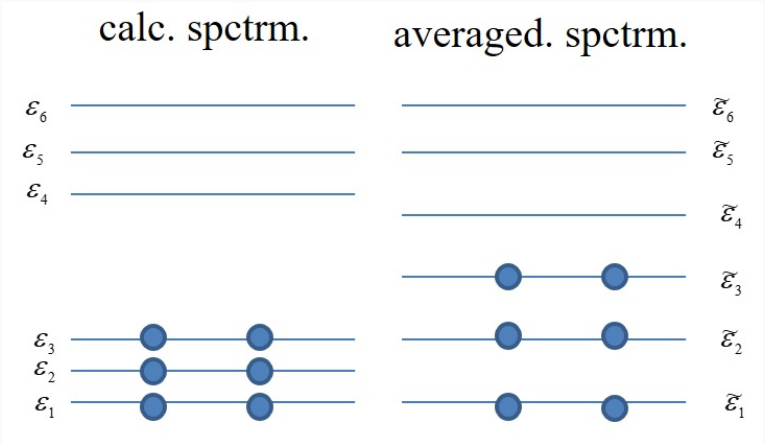

$$E_{calc} = 2(\varepsilon_1 + \varepsilon_2 + \varepsilon_3) \qquad E_{av} = 2(\tilde{\varepsilon}_1 + \tilde{\varepsilon}_2 + \tilde{\varepsilon}_3)$$

$$E_{shell} = E_{calc} - E_{av}$$

Shell correction is added to the binding energy

Shell corrections E_{shell}

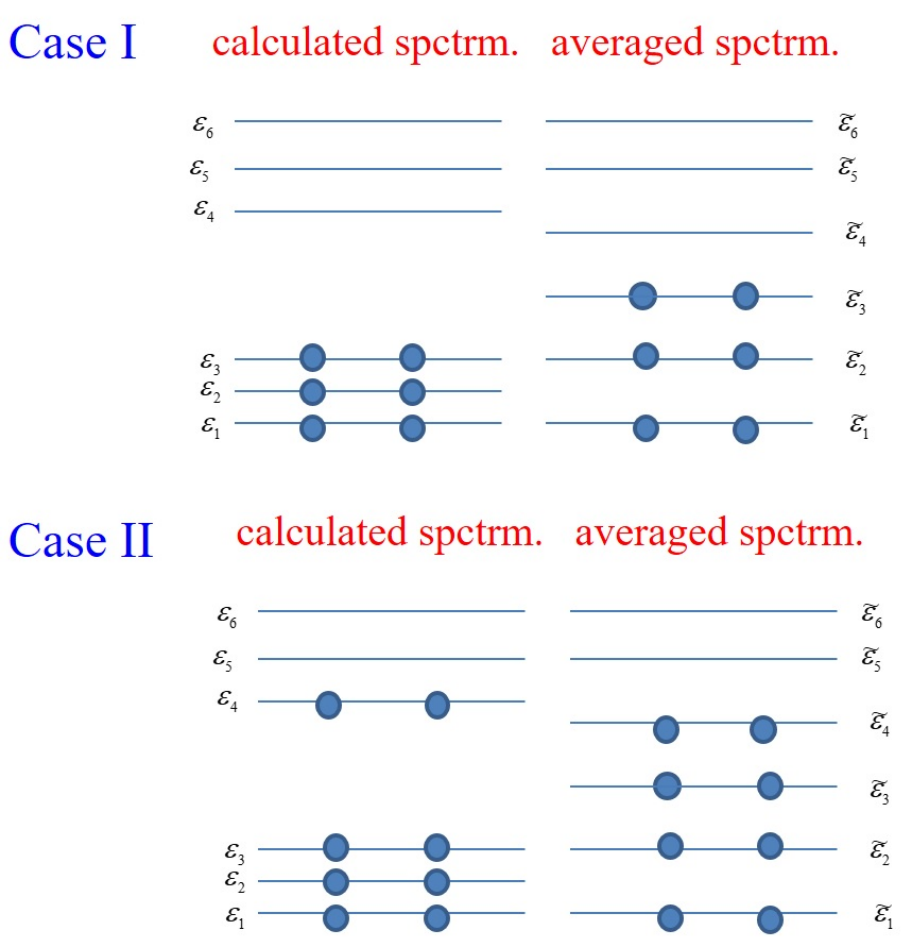

$$E_{shell} = E_{calc} - E_{av} < 0$$

Binding energy is increased

due to shell structure

$$E_{shell} = E_{calc} - E_{av} > 0$$

Binding energy is decreased

due to shell structure

Strutinsky method

$E_{shell} = E - \tilde{E}$

$$E = 2\int_{-\infty}^{\varepsilon_f} \varepsilon g(\varepsilon) d\varepsilon$$

$$\tilde{E} = 2\int_{-\infty}^{\tilde{\varepsilon}_f} \varepsilon \tilde{g}(\varepsilon) d\varepsilon.$$

$N = \int_{-\infty}^{\tilde{\varepsilon}_f} \tilde{g}(\varepsilon) d\varepsilon$

$$g(\varepsilon) = \Sigma_k \delta(\varepsilon - \varepsilon_k)$$

$$\tilde{g}(\varepsilon) = \frac{1}{\tilde{\gamma}} \int_{-\infty}^{+\infty} g(\varepsilon') f\left(\frac{\varepsilon - \varepsilon'}{\tilde{\gamma}}\right) d\varepsilon'$$

Strutinsky smoothing function: $f(x) = \frac{\exp\left(-x^2\right)}{\sqrt{\pi^2}} \sum_{k=0,2,\ldots}^{2m} c_k H_k(x)$.
$c_0 = 1$, and $c_{n+2} = -c_n/(n+2)$

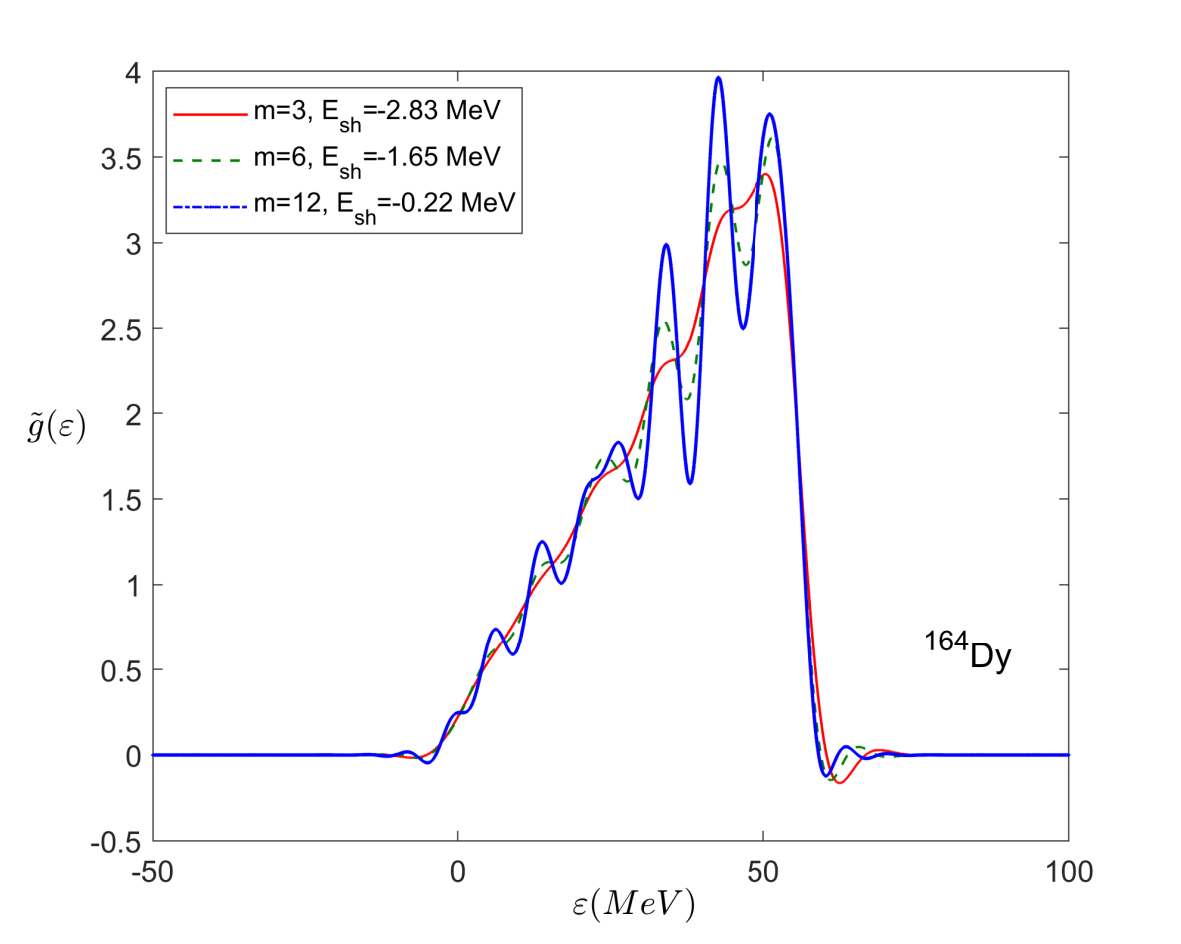
m=3, E_sh=-2.83 MeV
m=6, E_sh=-1.65 MeV
m=12, E_sh=-0.22 MeV
$\tilde{g}(\varepsilon)$
$\varepsilon(MeV)$
^{164}Dy
4
3.5
3
2.5
2
1.5
1
0.5
0
-0.5
-50
0
50
100

Fission barriers in micro-macro model

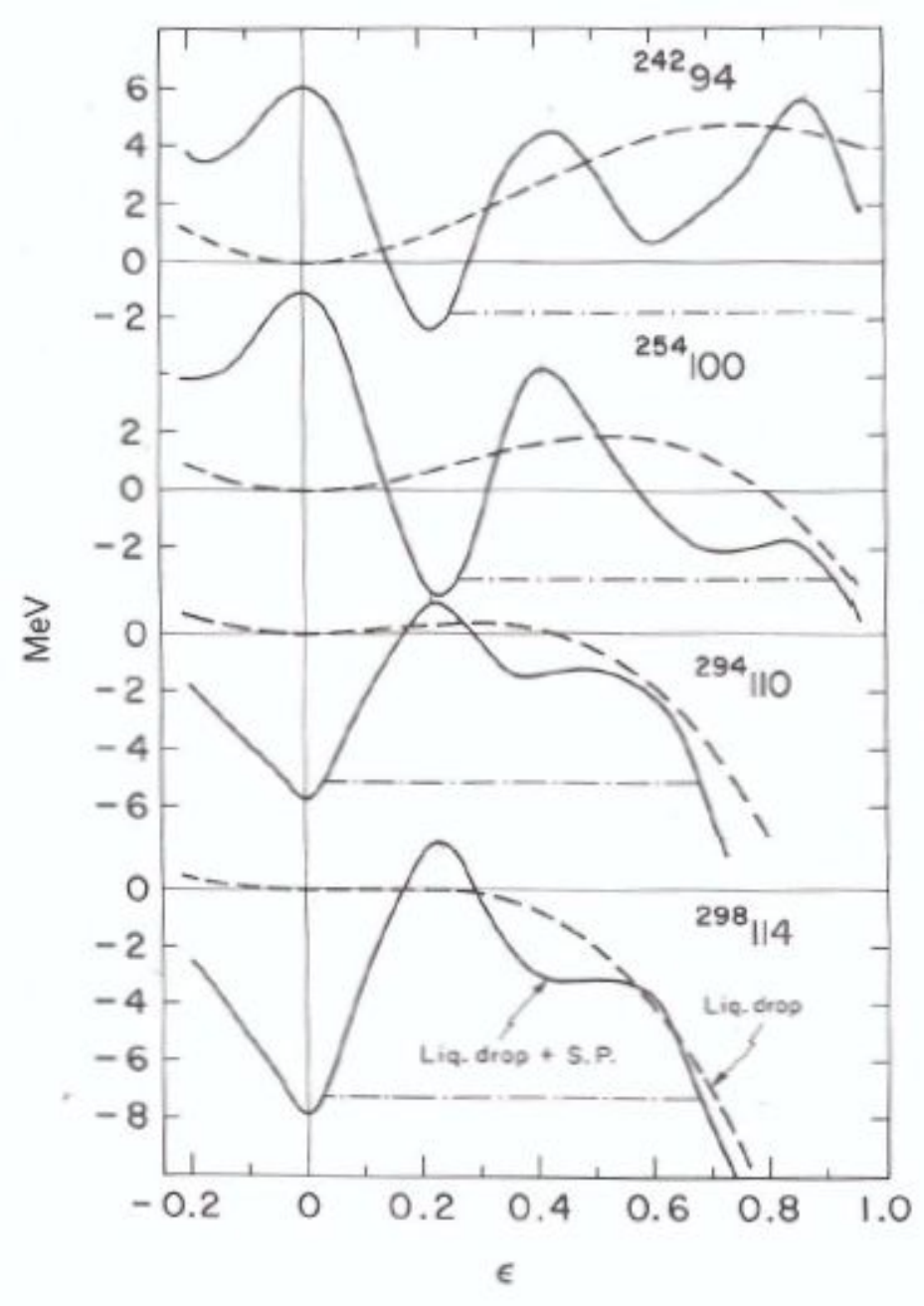

Statistical scission-point model

Statistical scission-point model

Only the last stage of fission (scission point) is considered. The scission configuration consists of the two well defined fragments in contact. After the scission no nuclear interaction occurs between the fragments.

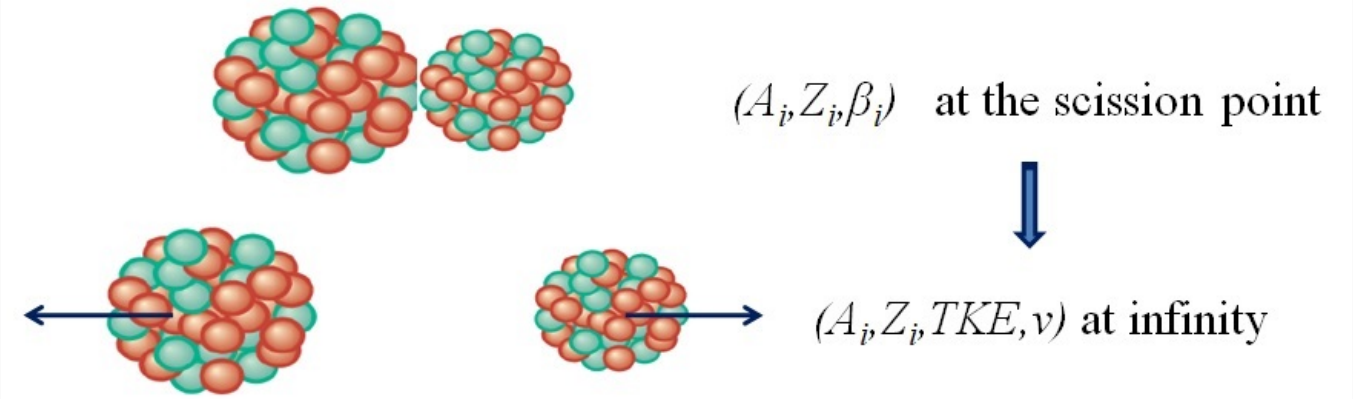

Advantages of the model

- Variation of N/Z ration in the fragments, hence, thorough account of shell structure in fragment
- No freedom in definition of the moment of neck rupture
- Simultaneous description of many fission observables

Comparison to other models:

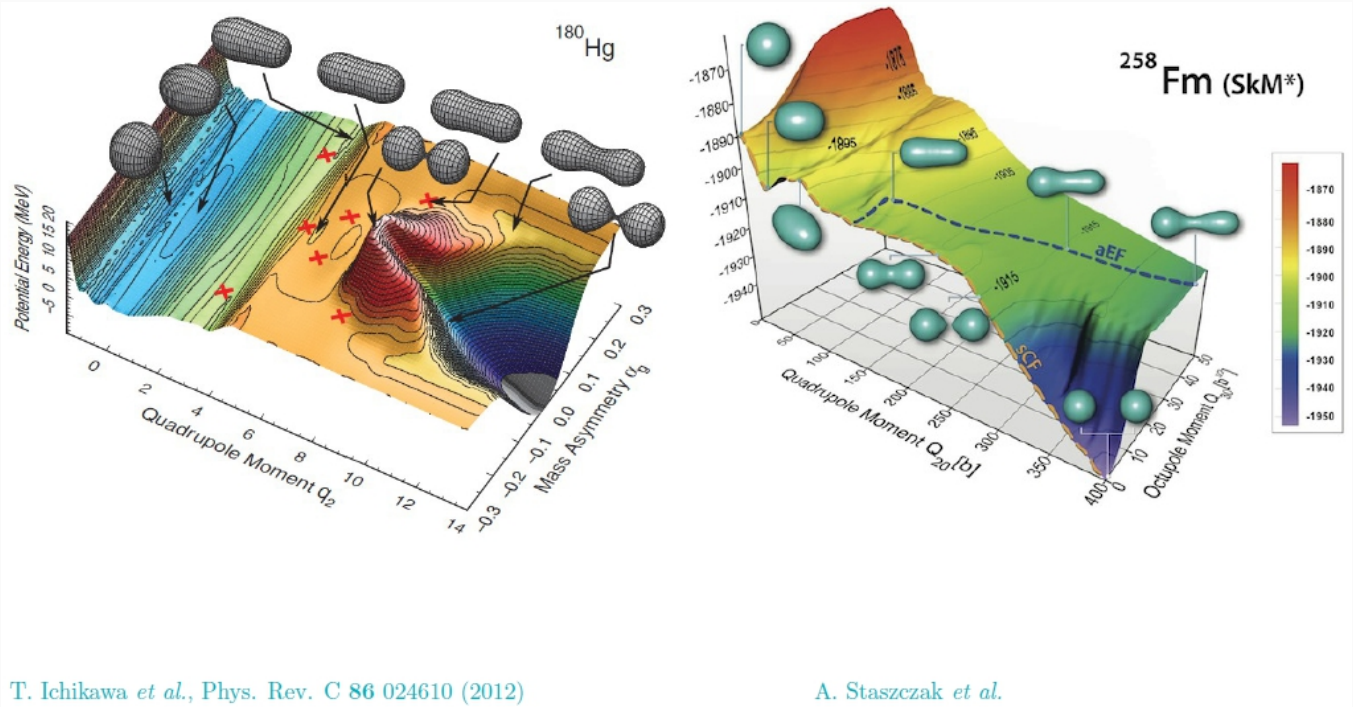

T. Ichikawa *et al.*, Phys. Rev. C **86** 024610 (2012)

A. Staszczak *et al.*

Main features of the model

- During the fission process the fragments of DNS interact intensively with each other but at the same time they keep their individuality.
- DNS can change by nucleon transfer between fragments. This transfer is ruled by potential energy of DNS.
- Due to fast establishing of thermal equilibrium the motion of DNS in mass and charge asymmetry coordinate has a statistical nature.

Statistical approach

The statistical equilibrium between all degrees of freedom (collective and intrinsic) is postulated at scission point.

The probability of realization of a particular scission configuration

$$(A_i, Z_i, \beta_i) \equiv (A_H, Z_H, \beta_H) + (A_L, Z_L, \beta_L)$$

is defined by the value of its potential energy with the Boltzmann factor:

$$P(A_i, Z_i, \beta_i) \sim \exp\left[-\frac{U(A_i, Z_i, \beta_i)}{T}\right]$$

Driving potential

Potential energy of the dinuclear system at the scission point as a function of mass asymmetry $\eta = \frac{A_H - A_L}{A_H + A_L}$

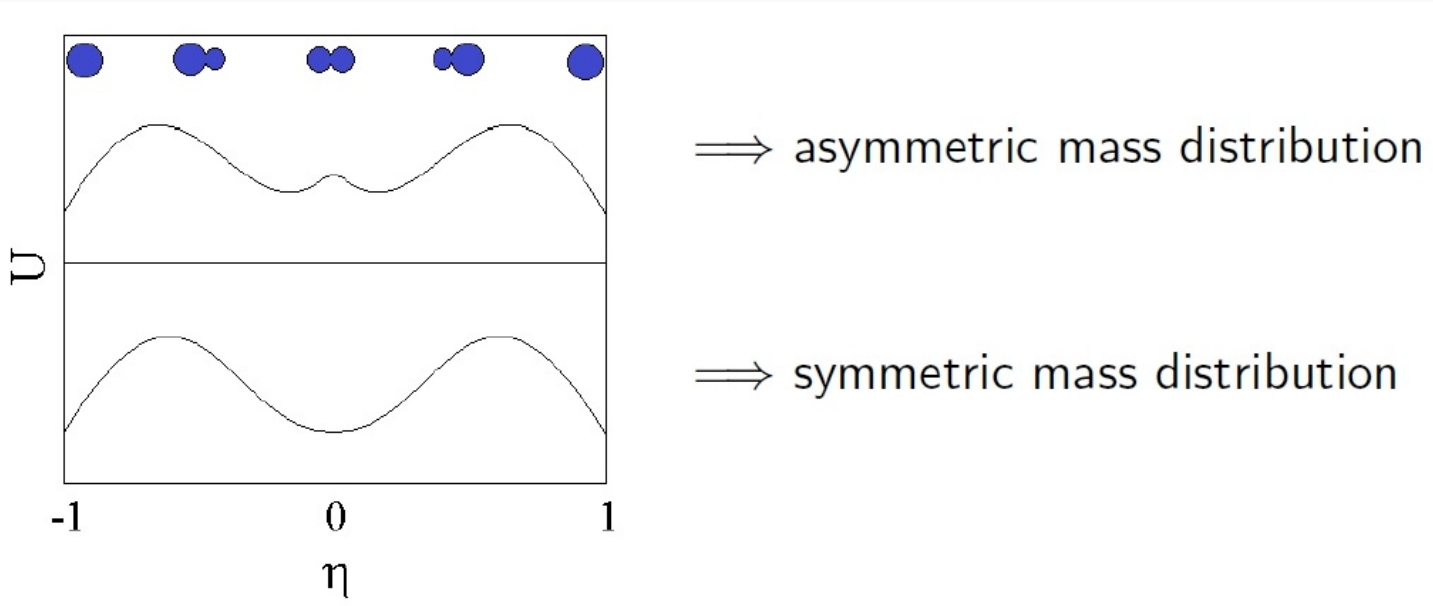

Potential energy of binary system

$$\beta_i = \frac{c_i}{a_i}, \qquad i = L, H$$

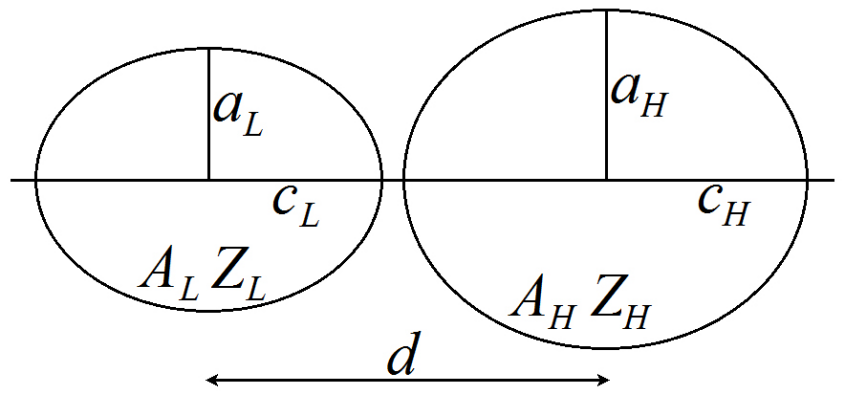

$$U_{DNS}(\beta_L, \beta_H, d) = \sum_{i=L,H} [U_i^{LD}(\beta_i) + \delta U_i^{sh}(\beta_i)] + V^C(\beta_L, \beta_H, d) + V^N(\beta_L, \beta_H, d)$$

- U_{LD}: Liquid-drop energy
- δU_H^{sh}: Shell correction
- V^C: Coulomb interaction
- V^N: Nuclear interaction

$$E^* = E^*_{comp} + U_{comp} - U_{sc}, \qquad T = \sqrt{E^*/a}, \qquad a = A/12$$

A.V. Andreev et al., EPJ A **30**, 579 (2006).

Macroscopic energy of DNS fragments

Coulomb energy:

$$U_i^C(A_i, Z_i, \beta_i) = \frac{3}{5}\frac{(Z_i e)^2}{R_{0,i}}\frac{\beta_i^{1/3}}{\sqrt{\beta_i^2 - 1}}\ln\left(\beta_i + \sqrt{\beta_i^2 - 1}\right)$$

$$R_{0,i} = 1.2249 A_i^{1/3}$$

Surface energy:

$$U_i^S(A_i, Z_i, \beta_i) = \sigma_i S_i,$$

$$\sigma_i = 0.9517(1 - 1.7826(N_i - Z_i)^2/A_i^2)\ \mathrm{MeV/fm^2}$$

Symmetry energy:

$$U_i^{Sym}(A_i, Z_i) = 27.612\frac{(N_i - Z_i)^2}{A_i}\ \mathrm{MeV}$$

Nuclear interaction energy

Double folding potential: (G. G. Adamian *et al.*, IJMPE **5**, 191 (1996).)

$$V^N(d) = \int \rho_1(\mathbf{r}_1)\rho_2(\mathbf{d}-\mathbf{r}_2)F(\mathbf{r}_1-\mathbf{r}_2)\mathrm{d}\mathbf{r}_1\mathrm{d}\mathbf{r}_2,$$

with the density-dependent forces (Migdal forces):
A. B. Migdal, *Theory of finite Fermi Systems...* (Nauka, Moscow, 1982).

$$F(\mathbf{r}_1-\mathbf{r}_2) = C_0\left(F_{in}\frac{\rho_0(\mathbf{r}_1)}{\rho_{00}} + F_{ex}\left(1-\frac{\rho_0(\mathbf{r}_1)}{\rho_{00}}\right)\right)\delta(\mathbf{r}_1-\mathbf{r}_2),$$

$F_{in,ex} = (f_{in,ex} + f'_{in,ex}\tau_\mathbf{1}\cdot\tau_\mathbf{2}) + (g_{in,ex} + g'_{in,ex}\tau_\mathbf{1}\cdot\tau_\mathbf{2})\sigma_\mathbf{1}\cdot\sigma_\mathbf{2}$

$C_0 = 300\ \mathrm{MeV\ fm}^3,\ f_{in,ex} = 0.09(-2.59),\ f'_{in,ex} = 0.42(0.54)$

$$\rho_0(\mathbf{r}) = \rho_1(\mathbf{r}) + \rho_2(\mathbf{r}).$$

Densities are in the form of Fermi distribution.

Interaction potential of DNS fragments

$$V^N(d) = C_0 \left\{ \frac{F_{in} - F_{ex}}{\rho_{00}} \left(\int \rho_1^2(\mathbf{r})\rho_2(\mathbf{r}-\mathbf{d})\mathrm{d}\mathbf{r} + \int \rho_1(\mathbf{r})\rho_2^2(\mathbf{r}-\mathbf{d})\mathrm{d}\mathbf{r} \right) + F_{ex} \int \rho_1(\mathbf{r})\rho_2(\mathbf{r}-\mathbf{d})\mathrm{d}\mathbf{r} \right\}, \quad F_{in,ex} = f_{in,ex} + f'_{in,ex} \frac{N_1 - Z_1}{A_1} \frac{N_2 - Z_2}{A_2}$$

DNS stays close to the touching configuration in the pocket created by the interplay between nuclear and Coulomb interactions

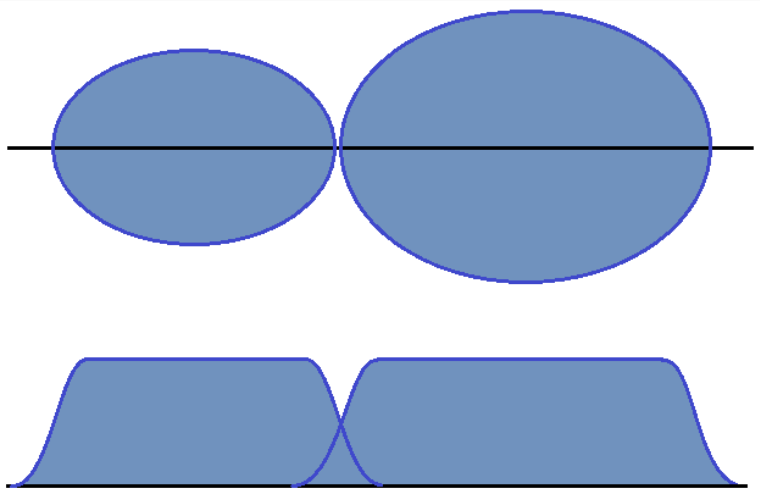

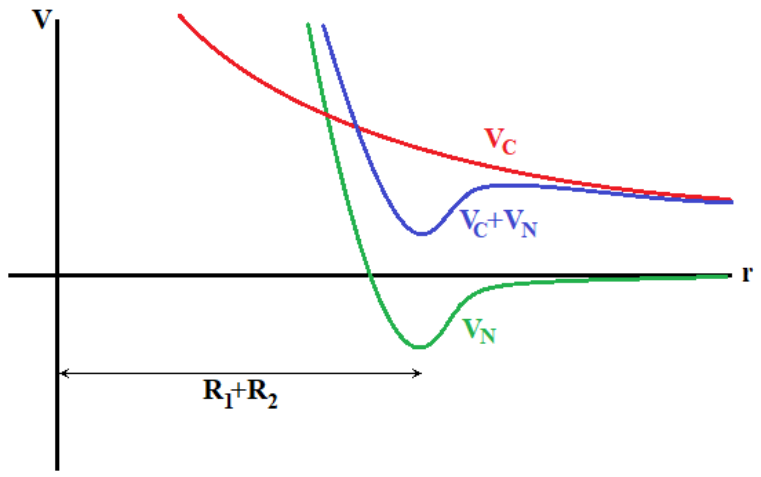

Potential energy of DNS as a function of the fragment deformations

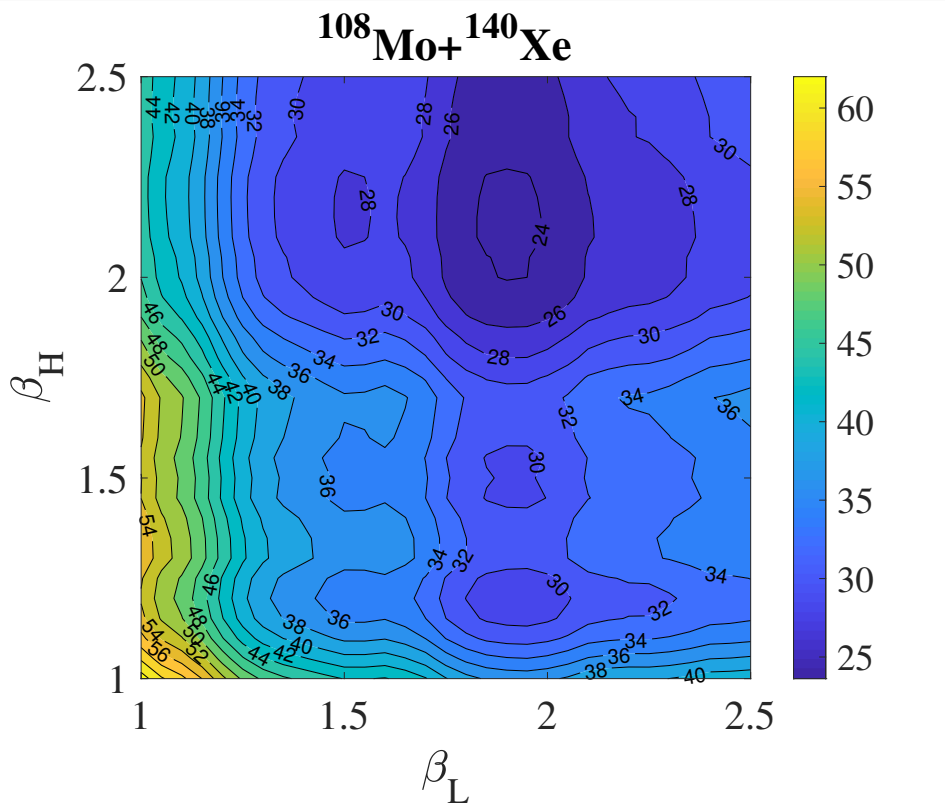

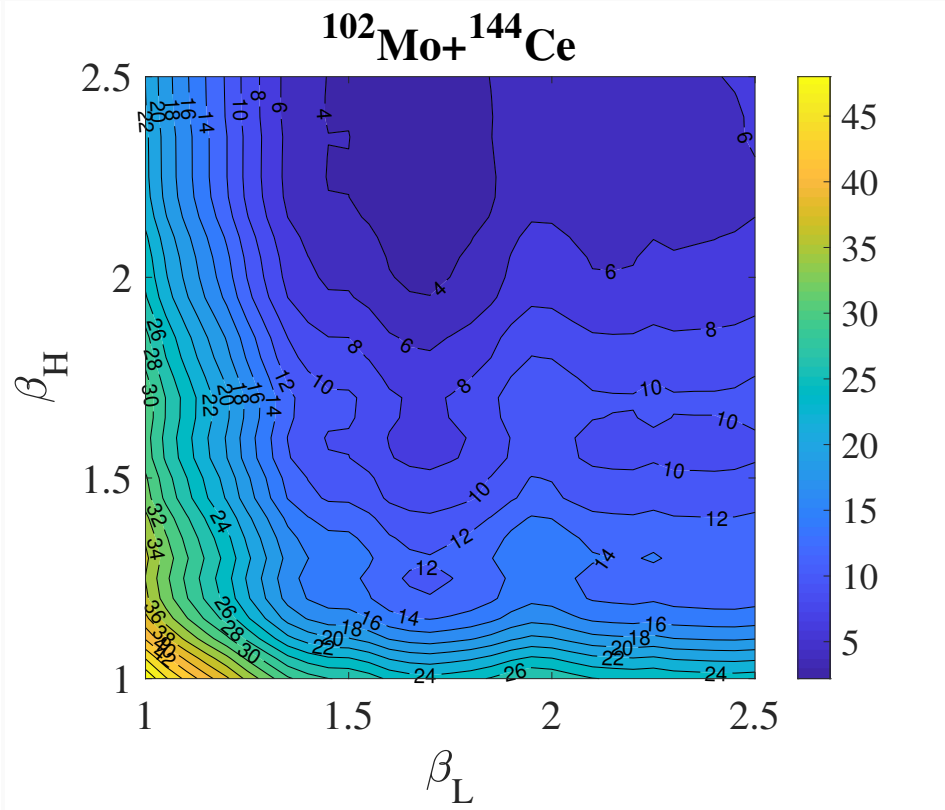

Complex structure of the PES (one or several local minima) is due to the shell correction of fragments.

Damping of shell corrections with excitation

$$\delta U_i^{sh}(E_i^*) = \delta U_i^{sh}(0)\ \exp\left(-\frac{E_i^*}{E_D}\right), \quad E_D = 18.5\ \mathrm{MeV}$$

$^{106}\mathrm{Mo} + ^{146}\mathrm{Ba}$:

with shell corrections

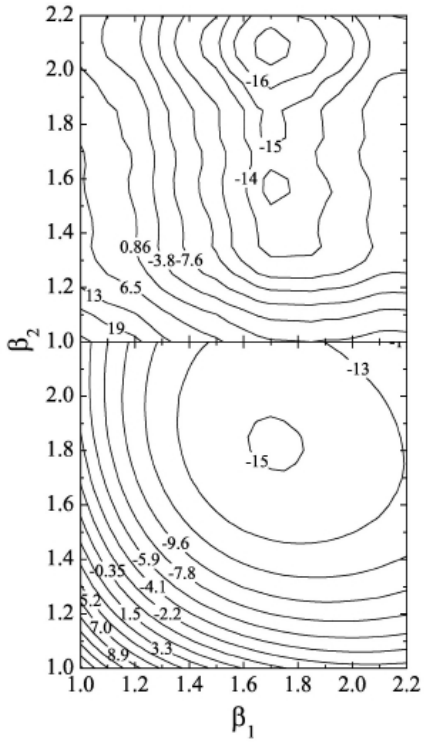

without shell corrections

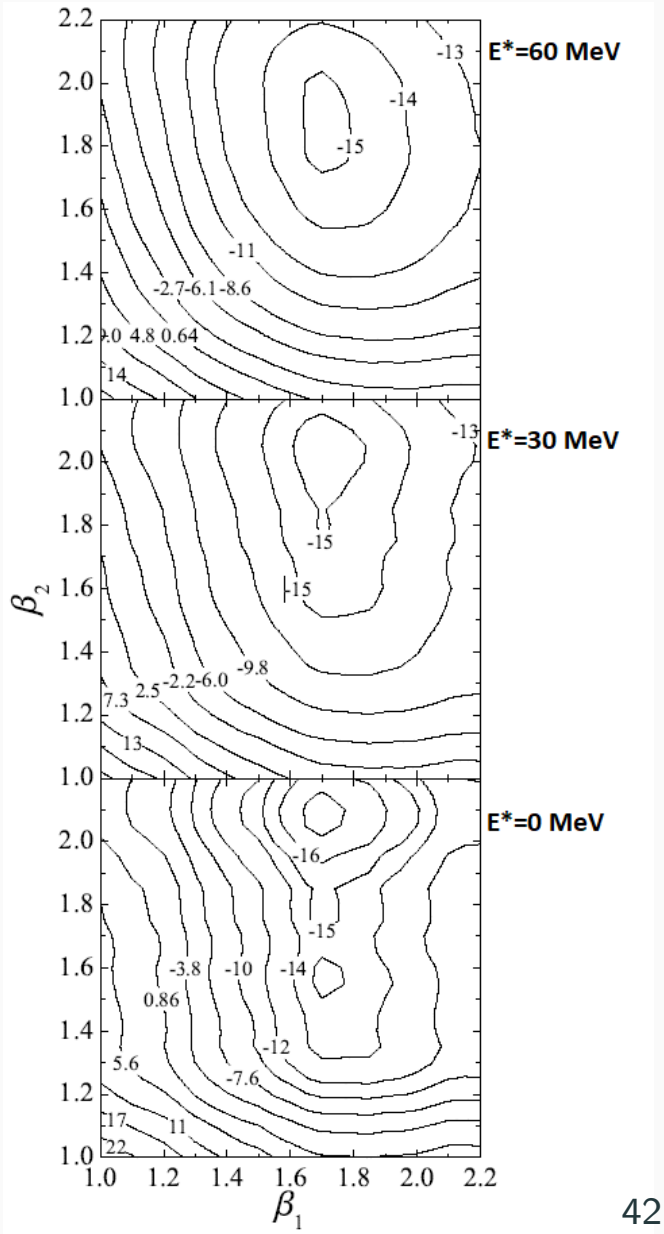

Potential energy of DNS as function of asymmetry

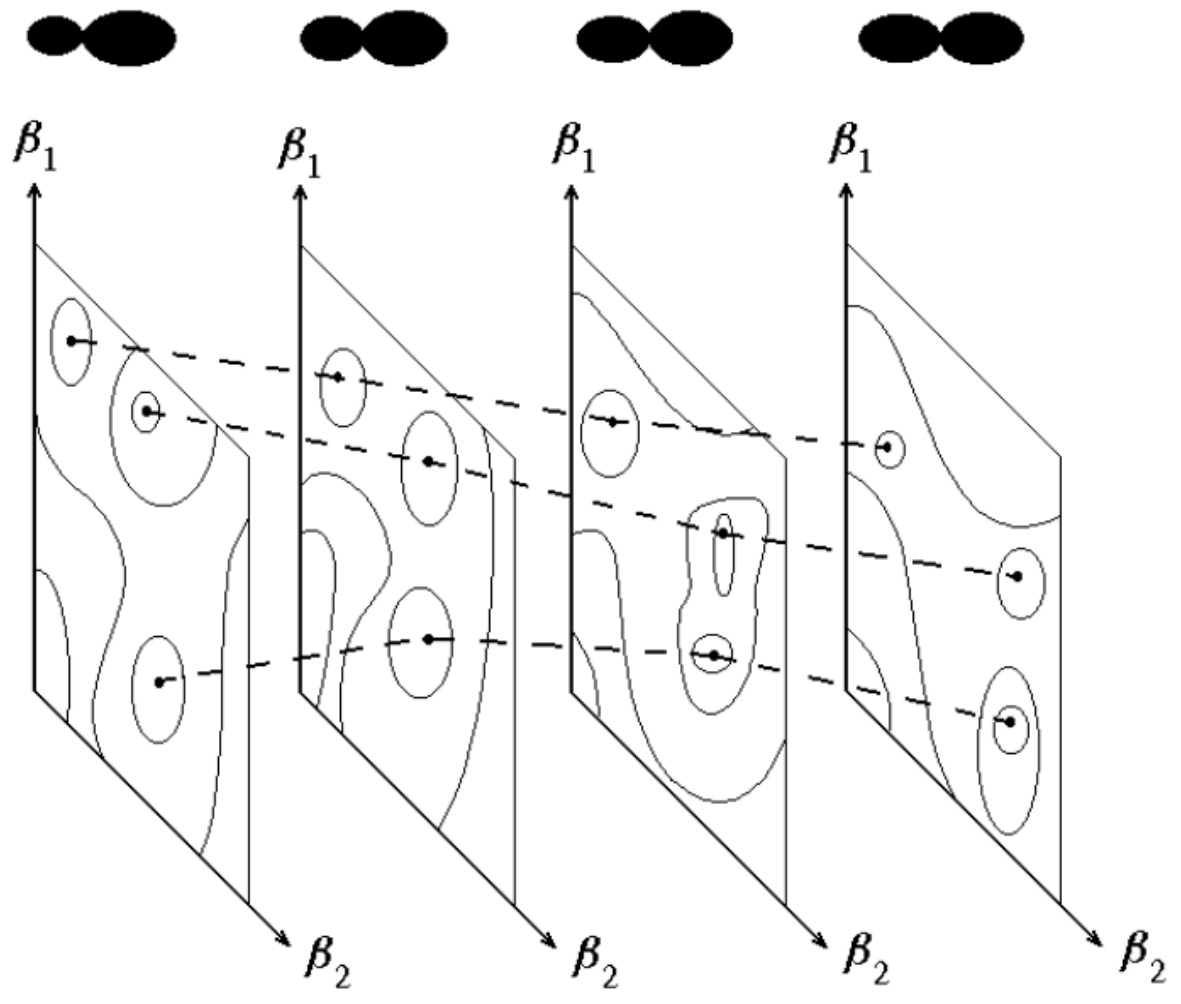

Mass and charge distributions

$$Y_L(A_L) = \frac{\sum_{Z_L} \int \exp\left[-\frac{U(A_i,Z_i,\beta_i)}{T}\right] d\beta_L d\beta_H}{N}$$

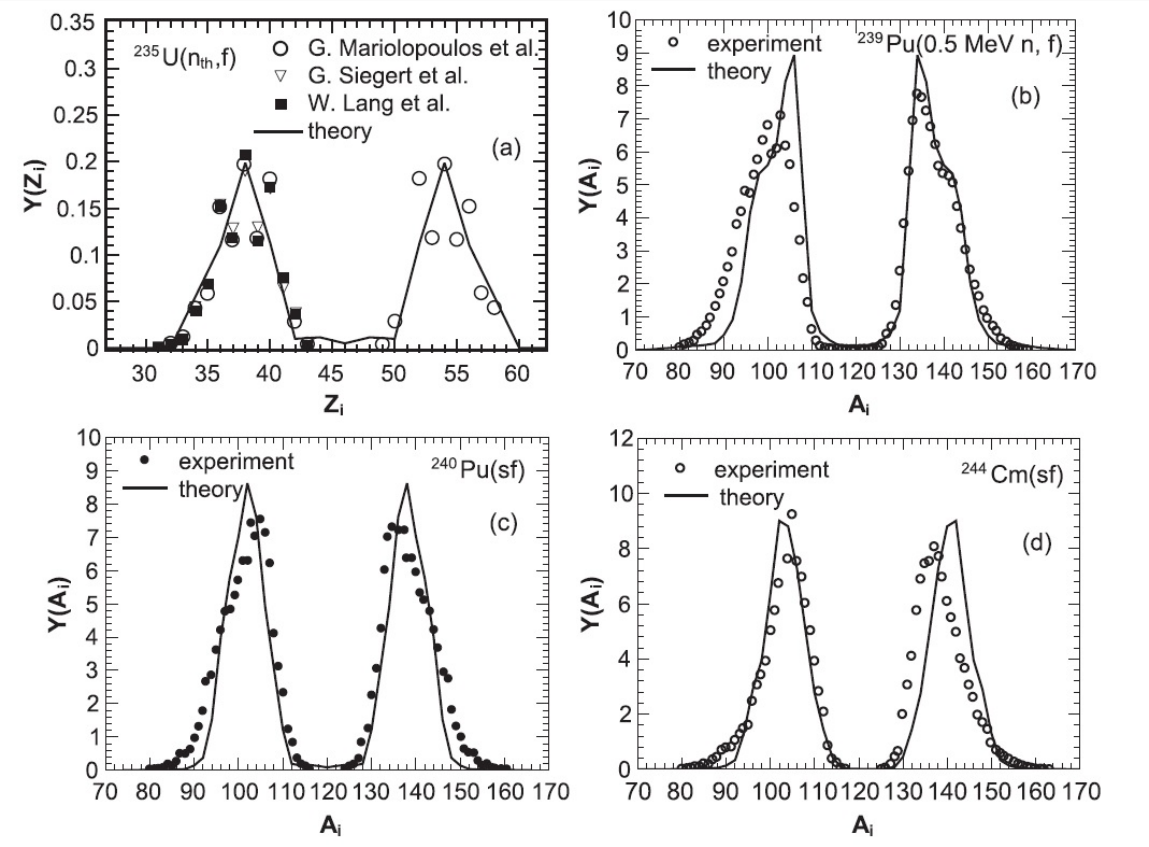

H. Pasca, et al., Phys. Rev. C 108, 014613 (2023).

Deformation dependent shell corrections

Change of "magic numbers" with deformation:

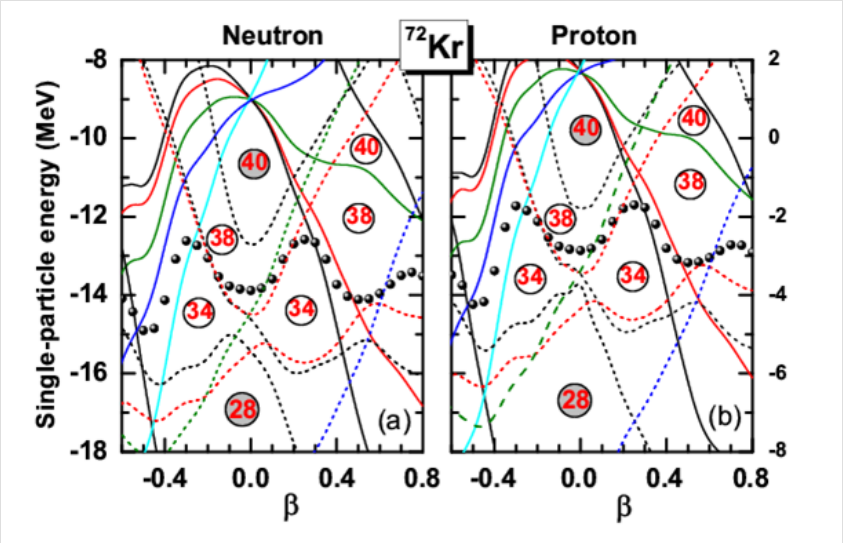

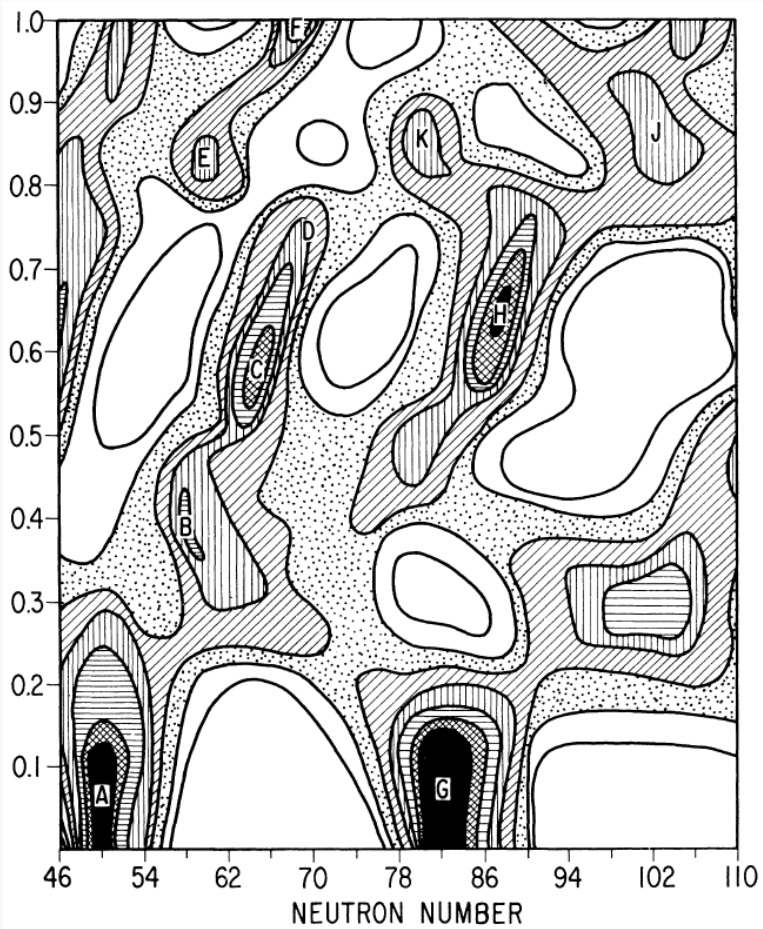

Energy balance

E^* - excitation energy of DNS

E_K - kinetic energy of the fragments

$Q = B_1 + B_2 - B_{COMP}$ - amount of energy released during fission

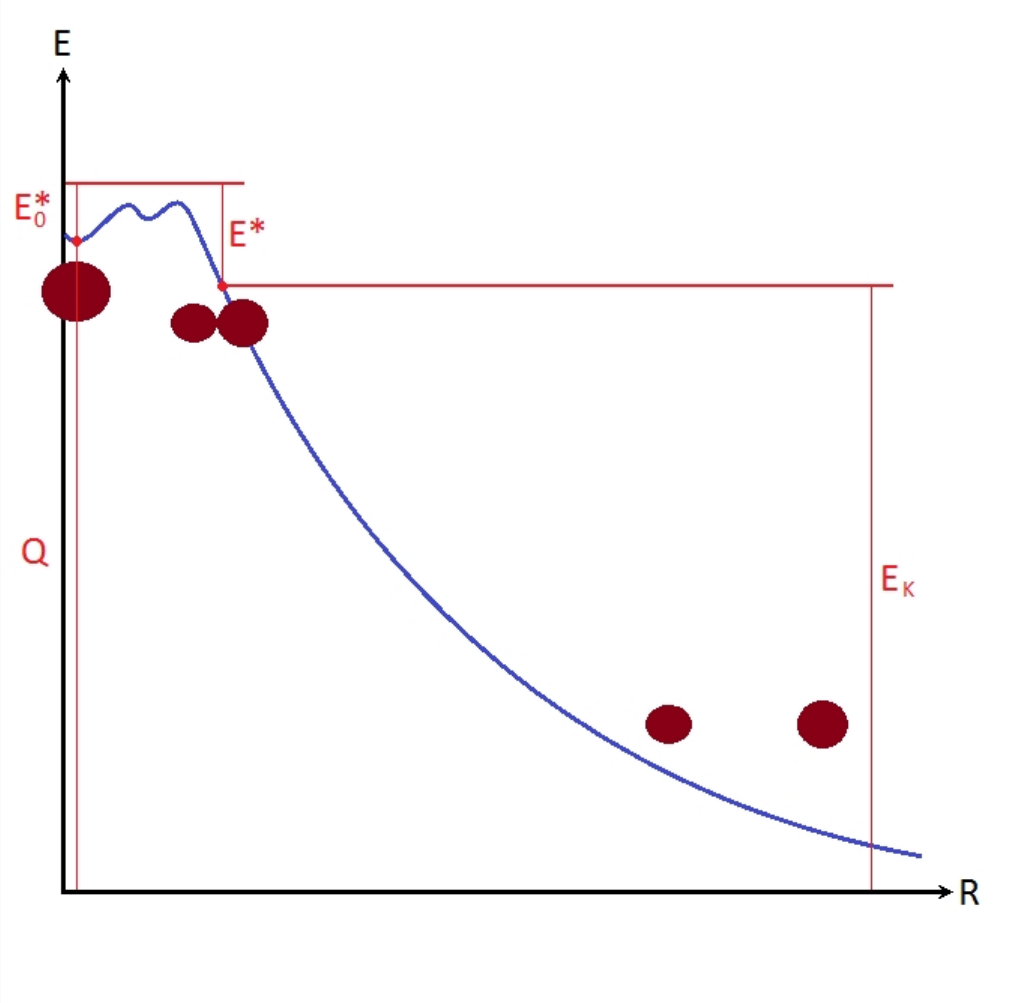

Total kinetic energy

$$TKE(A_i, Z_i, \beta_i) = V^C(A_i, Z_i, \beta_i) + V^N(A_i, Z_i, \beta_i)$$

TKE(^{76}Se+^{104}Pd) in MeV as a function of deformations

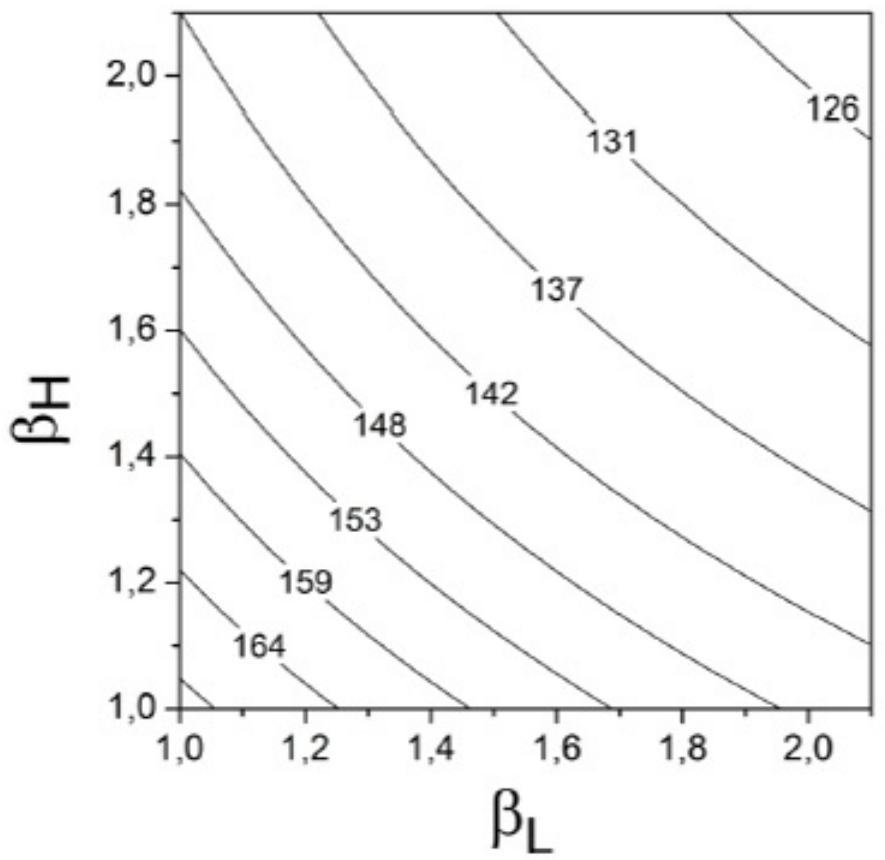

Total kinetic energy distribution

$$\langle \mathrm{TKE} \rangle (A_i) = \frac{1}{N} \sum_{Z_i} \int \mathrm{TKE}(A_i, Z_i, \beta_i) \exp \left[- \frac{U(A_i, Z_i, \beta_i)}{T} \right] d\beta_L d\beta_H$$

$$\overline{\mathrm{TKE}} = \frac{1}{N'} \sum_{A_i, Z_i} \int \mathrm{TKE}(A_i, Z_i, \beta_i) \exp \left[- \frac{U(A_i, Z_i, \beta_i)}{T} \right] d\beta_L d\beta_H$$

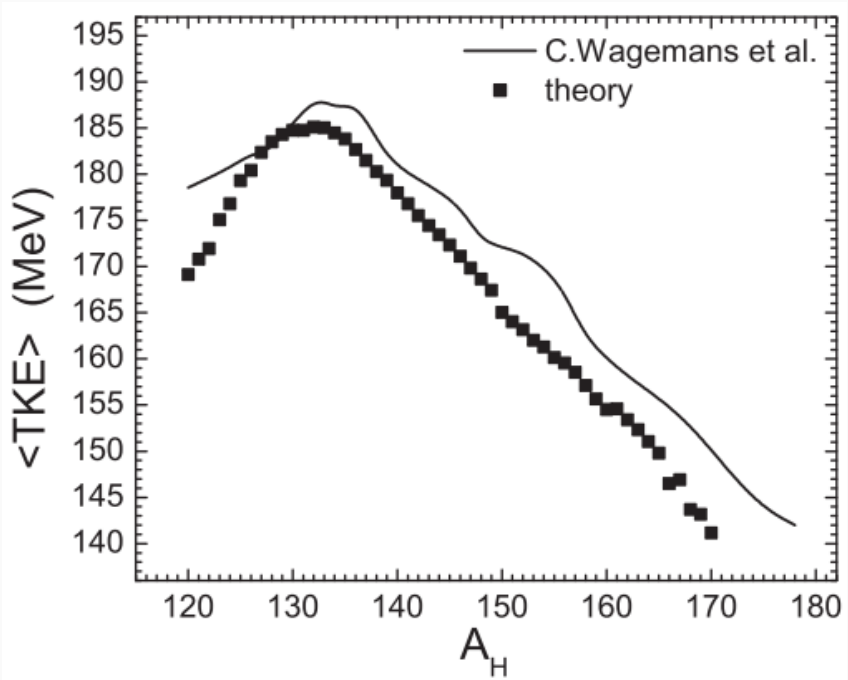

FIG. 13. The calculated (solid line) average total kinetic energies of fission fragments in the ^{239}Pu(n_{th},f) reaction versus fragment mass. The experimental data (symbols) are from Ref. [27].

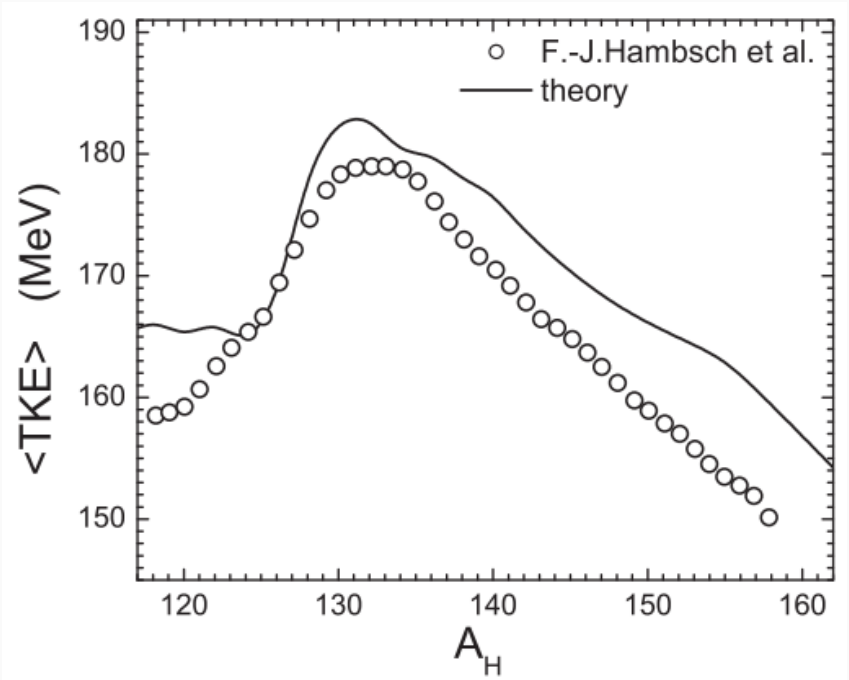

Neutron multiplicity

After splitting of DNS, fragments return to their ground state releasing energy stored in deformation as an excitation energy.

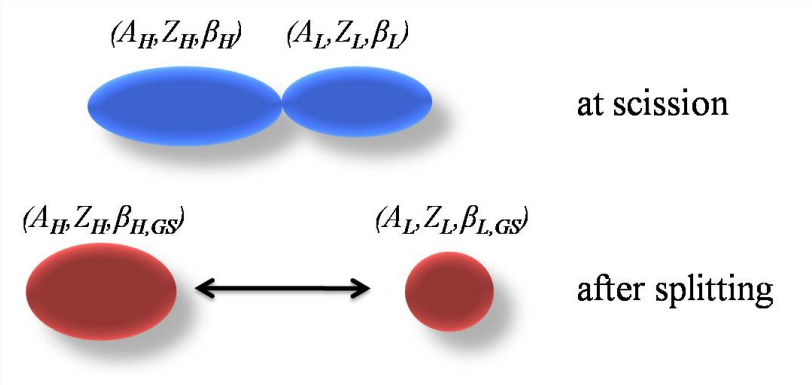

$$E_H^* = \frac{A_H}{A_H + A_L} E^* + E_H^{def}$$
$$E_L^* = \frac{A_L}{A_H + A_L} E^* + E_L^{def}$$

$$E_i^{def} = \left[U_i^{LD}(\beta_i) + \delta U_i^{sh}(\beta_i)\right] - \left[U_i^{LD}(\beta_{i,GS}) + \delta U_i^{sh}(\beta_{i,GS})\right]$$

The fragments cool down by emission of neutrons

Neutron multiplicity

Excitation energy distributions based on level densities:

$$E_H^* = \frac{a_H}{a_H + a_L} E^* + E_H^{def}$$

$$E_L^* = \frac{a_L}{a_H + a_L} E^* + E_L^{def}$$

Level density parameter:

$$a_i = \tilde{a}_i(A_i) \left(1 + \frac{1 - \exp\{-E_i^*/E_D\}}{E_i^*} \delta U_i^{sh} \right)$$

where the parameter $\tilde{a}_i(A_i)$ is taken proportional to A_i, and $E_D = 18.5$ MeV.

Neutron multiplicity from fragment (approximation):

$$n_i = \text{floor}\left[\frac{E_i^*}{B_n + 2T} \right], \qquad i = L, H$$

(*More accurate - step by step emission*)

Neutron multiplicity

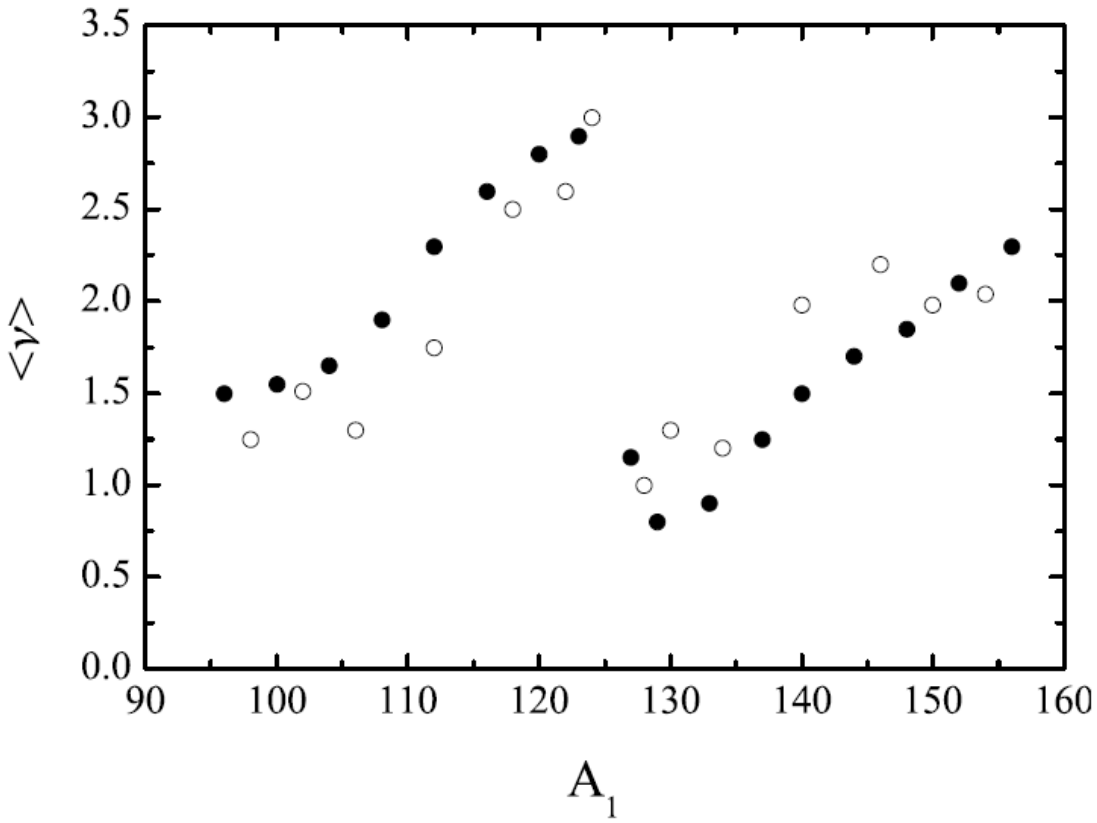

Fig. 7. Neutron multiplicity from individual fragments in the spontaneous binary fission of ^{252}Cf as a function of the fragment mass. The experimental data [1] and calculated results are presented by closed and open circles, respectively.

Dynamical calculations based on SPM

Measurements of neutron multiplicities at FLNR JINR

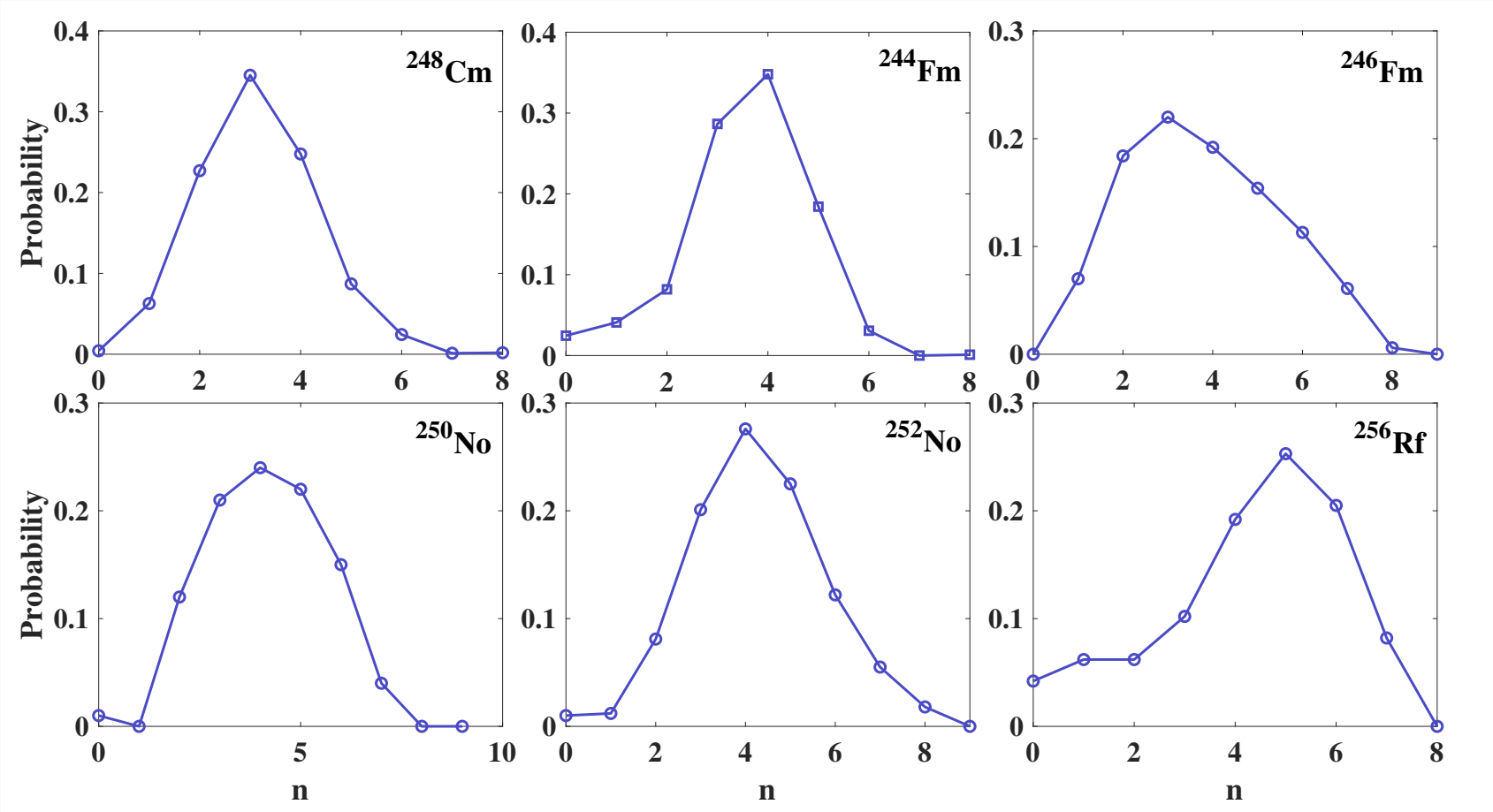

A.V. Isaev, et al., PLB **843**, 138008 (2023).

A. V. Isaev, EPJA, **58** 108 (2022).

R.S. Mukhin et al., Phys. Part. Nucl. Lett. 18(4), 439–444 (2021).

Mass distributions and neutron multiplicities in equilibrium

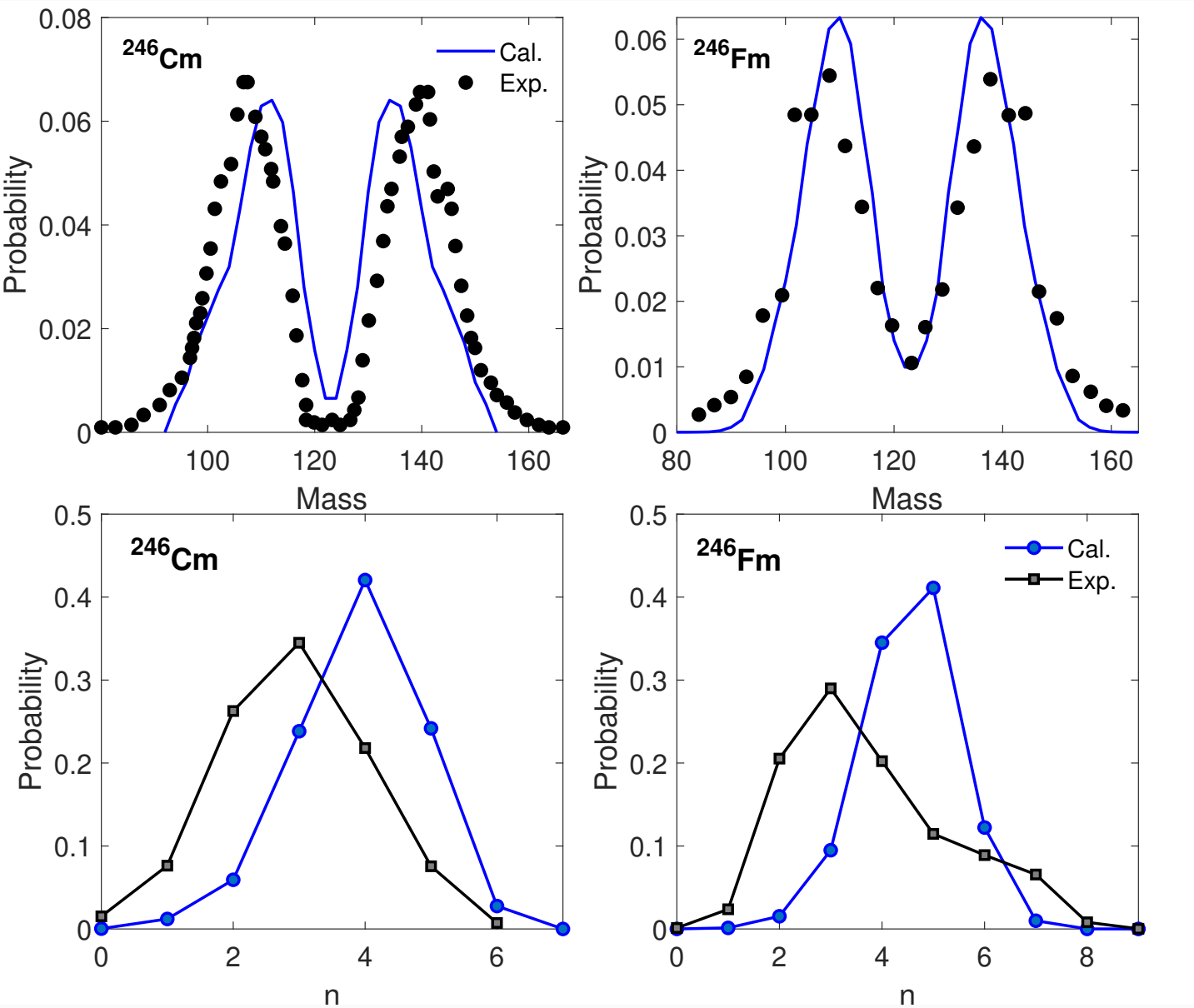

Evolution of fissile nucleus after crossing the fission barrier

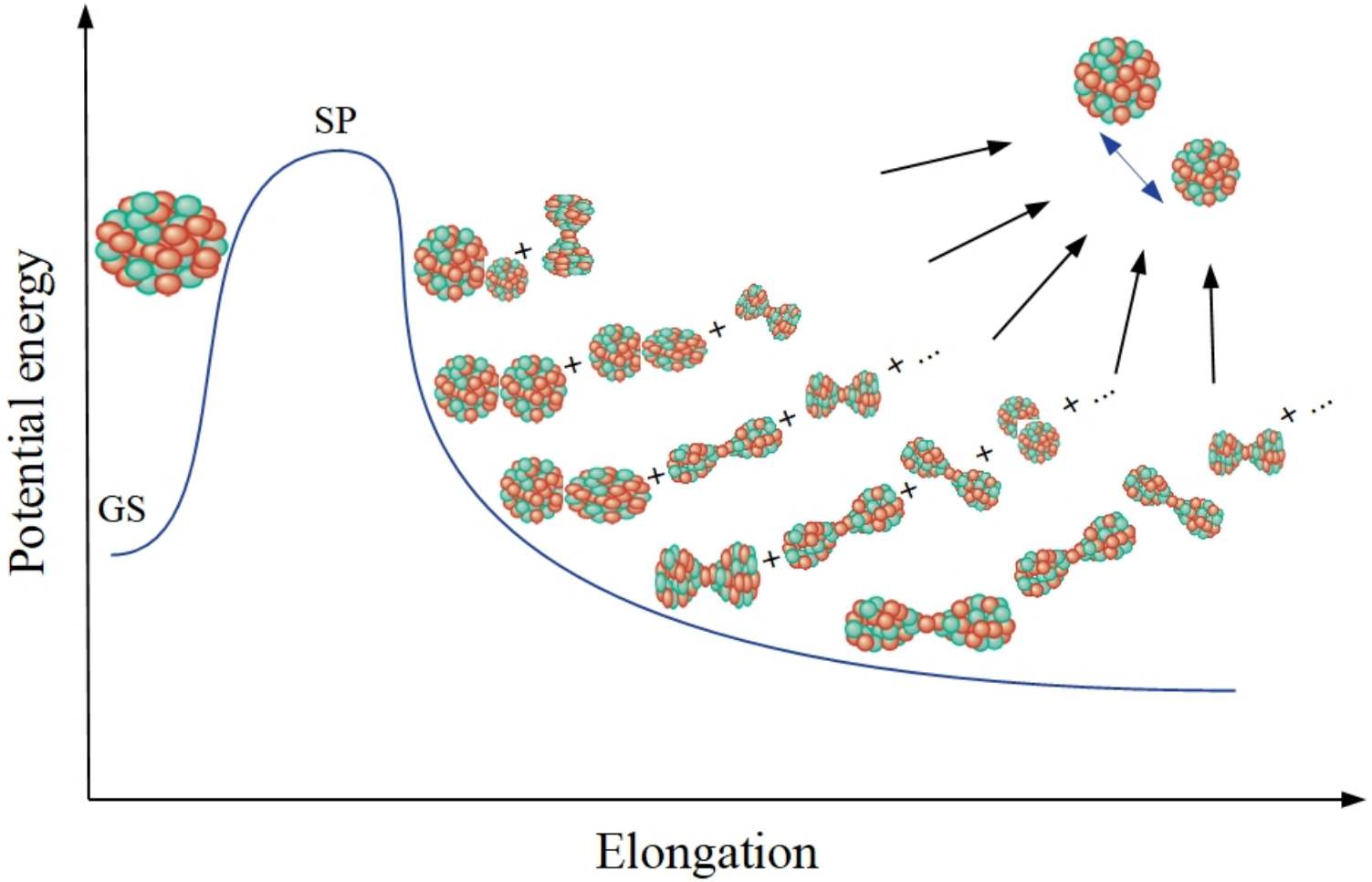

Dynamical calculation of fission yields

To describe neutron multiplicity, the evolution of the DNS distribution at scission point is treated as a random walk on the PES calculated in the ISP model in competition with the decay in relative distance.

$$\frac{\mathrm{d}}{\mathrm{d}t}P(n,t) = \sum_{n'}\left[\Lambda(n'|n)P(n',t) - \Lambda(n|n')P(n,t)\right] - \Lambda_{decay}(n)P(n,t)$$

Deformation space is discretized with constant step 0.05.

$$n = \{A_i, Z_i, \beta_i\}, \quad i = L, H$$

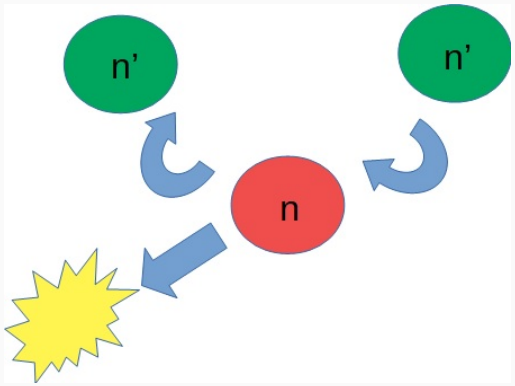

Potential energy of DNS as function of asymmetry

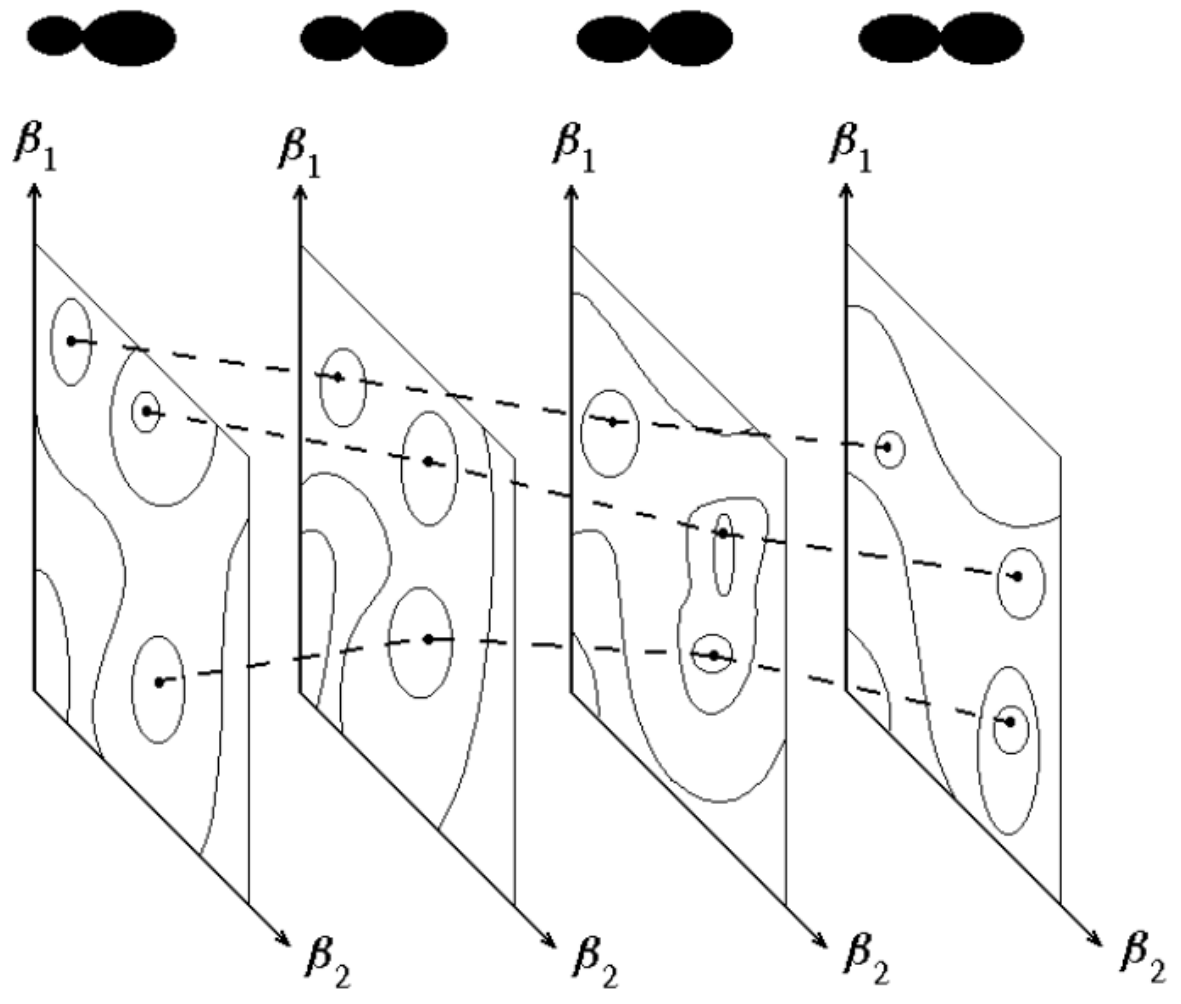

Transition probabilities

The macroscopic transition probabilities are taken in terms of the microscopic transition probabilities and of the level densities of the final state.

$$\Lambda(n|n') = \lambda_{nn'}\rho(E^*_{n'}, n'), \;\; \Lambda(n'|n) = \lambda_{n'n}\rho(E^*_n, n)$$

$$\lambda_{n'n} = \lambda_{nn'}$$

Only transitions to the neigboring states are considered:

$$\beta'_i = \beta_i \pm 0.05, \quad A'_i = A_i \pm 2$$

G.G. Adamyan, A.K. Nasirov, N.V. Antonenko, R.V. Jolos , Fiz. Elem. Chastits At.Yadra **25**, 1379 (1994).
L.G. Moretto and J.S. Sventek, Phys. Lett. B **58**, 26 (1975).

Transition probabilities

Microscopic transition probabilities are

$$\lambda_{n'n} = \lambda_{nn'} = \lambda^{(i)} / \sqrt{\rho(n')\rho(n)}; \;\; i = A, \beta$$

- $\lambda^{(A)}$ describes the transmission of nucleons between the fragments.
- $\lambda^{(\beta)}$ describes the change of deformation of fragments.
- $\lambda^{(A)}$ and $\lambda^{(\beta)}$ are treated as parameters of the model

$$\rho(E^*, n) = \int \rho_H(E^* - \varepsilon)\rho_L(\varepsilon)\mathrm{d}\varepsilon \propto \rho_H\left(\frac{A_H}{A_H + A_L}E^*\right)\rho_L\left(\frac{A_L}{A_H + A_L}E^*\right)$$

$\rho_{H,L}$ are calculated with the Fermi-gas model

Level density explanation

Level density of excited nucleus is the number of excited states per unit interval of excitation energy:

$$\rho(E^*) = \frac{dN(E^*)}{dE^*}$$

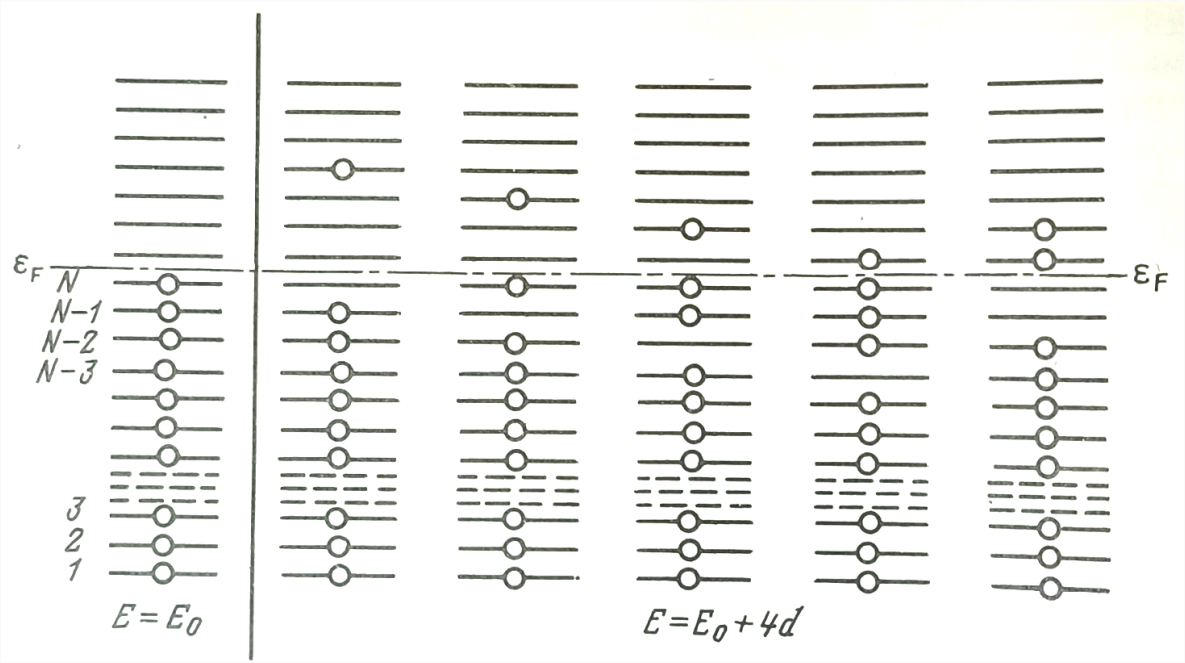

Energy distance between the levels: d [MeV]

Density of single-particle states: $g = \frac{1}{d}$ [MeV^{-1}]

Number of excited states at $E^* = 4d$: 5

Density of excited states:

$$\rho(E^* = 4d) = \frac{5}{d} = 5g$$

Fermi-gas model:

Non-interaction fermions in the potential well with rigid walls.
Equidistant spectrum with single-particle level density **g**.

$$\rho(E^*) = \frac{\exp[2\sqrt{aE^*}]}{\sqrt{48}E^*}$$

Level density parameter:

$$a = \frac{\pi^2}{6}g, \qquad T = \sqrt{\frac{E^*}{a}}$$

For real nuclei: $a = A/8...A/14$

Constant temperature model (for small excitations):

$$\rho(E^*) = \frac{\exp[E^*/T]}{T}$$

Decay probabilities

$$\Lambda_{decay}(n) = \lambda_d \rho_B(E^* - V_B, n)$$

$$\lambda_d = \begin{cases} 1/\sqrt{\rho_B(n)\rho(n)}, & \text{if } (E^* > V_B) \\ 0, & \text{if } (E^* < V_B) \end{cases}$$

$\rho_B(n)$ – level density at the barrier;

$\rho(n)$ – level density at the minimum of the pocket.

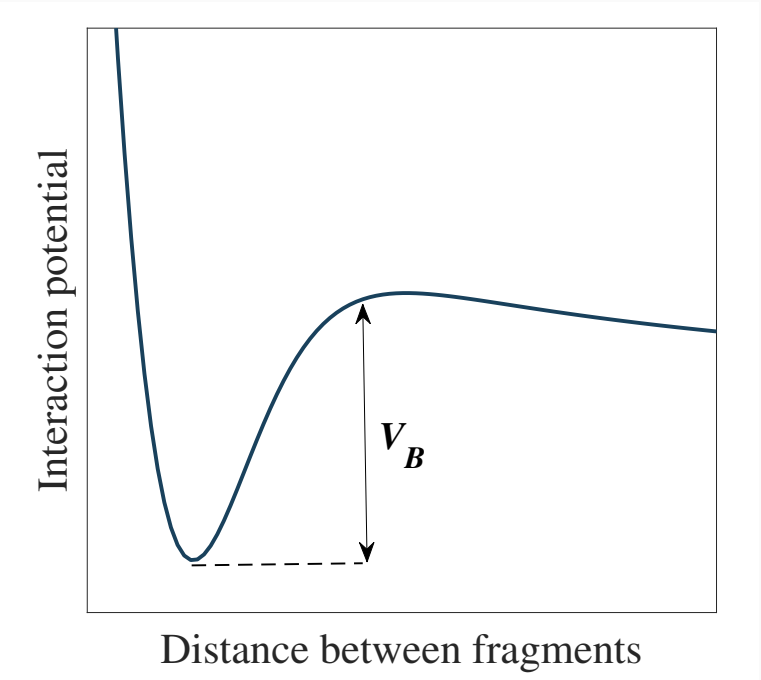

Choice of distribution of initial states

We choose the systems whose quadrupole moment lies in the interval of 10% around the value of quadrupole moment of ellipsoid with axis ratio $a : b$.

$Q_2^{ellips} \sim a : b$

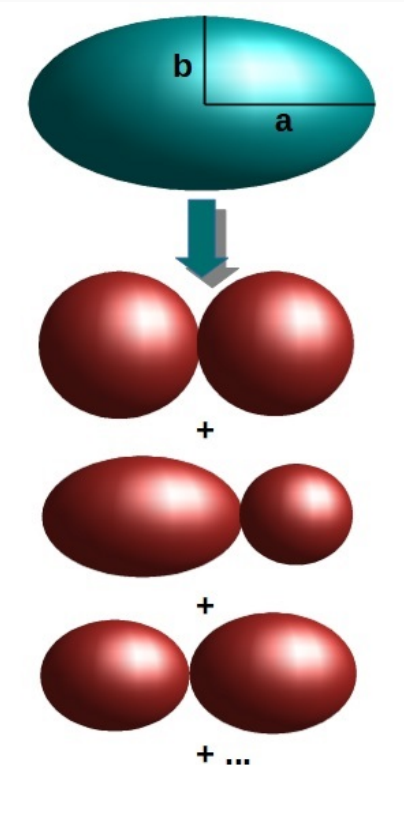

$Q_2 \sim Q_2^{ellips} \pm 10\%$

- **Probability of each DNS is taken as**

$$P_{init}\{N_i, Z_i, \beta_i\} \sim \rho\{N_i, Z_i, \beta_i\}(E^*)$$

- **Quadrupole moment of DNS is given as**

$$Q_2(\xi, d) = A\xi(1 - \frac{\xi}{2})d^2 + Q_2(A_L) + Q_2(A_H)$$

$$\xi = \frac{2A_L}{A_L + A_H}$$

Various calculations show that nucleus can be presented as a DNS around $Q_2^{ellips} \sim 3 : 1$.

^{256}Rf: Neutron multiplicity

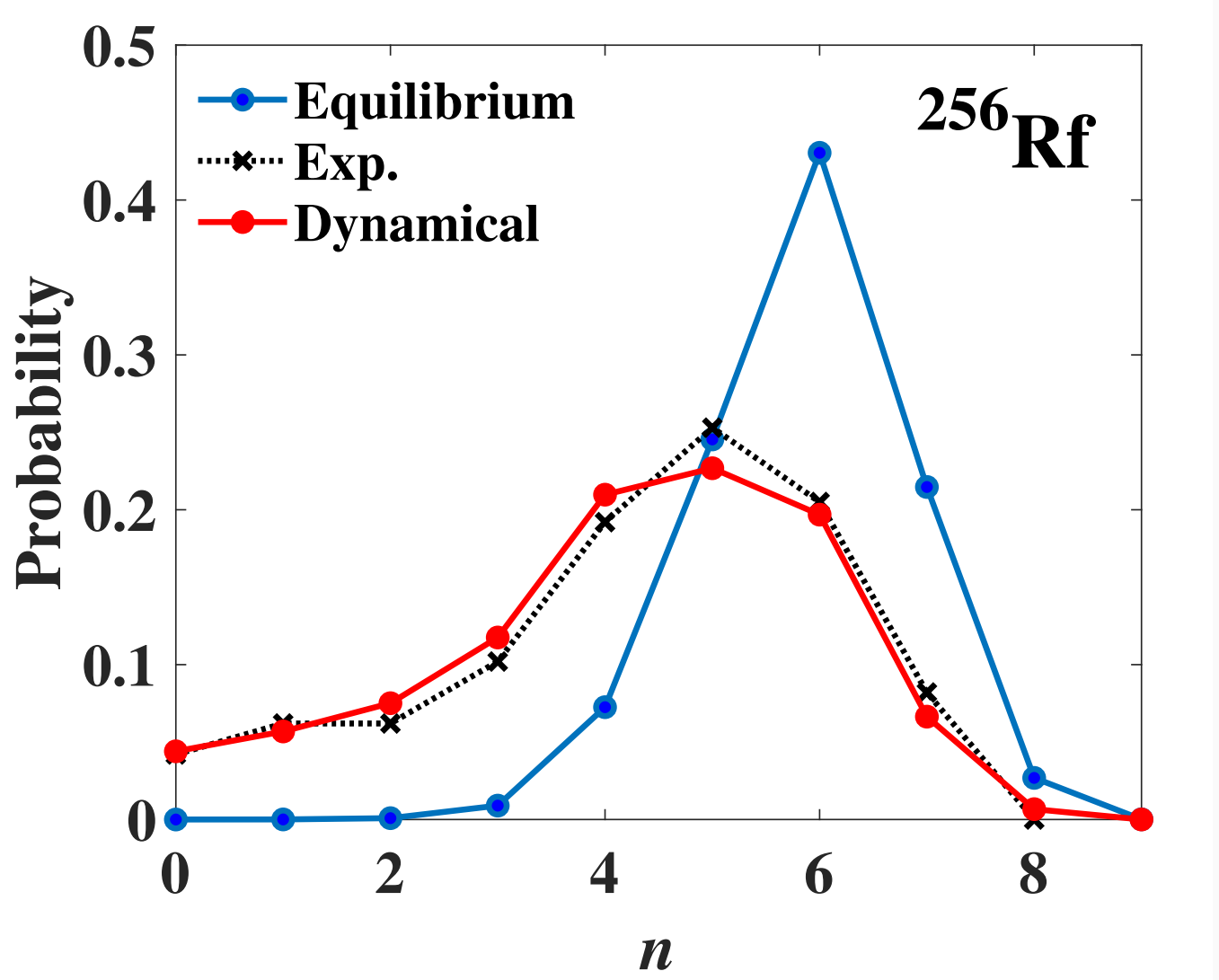

Parameters:

$\lambda^{(A)} = 1.85$

$\lambda^{(\beta)} = 1.4$

$Q_{init} \sim 2.8 : 1$

A.V. Isaev, et al., PLB **843**, 138008 (2023)

^{256}Rf: Mass distribution

solid line – overall;
squares: 0n – 1n;
circles: 2n – 3n;
triangles: 4n – 5n
rhombus: 6n – 9n.

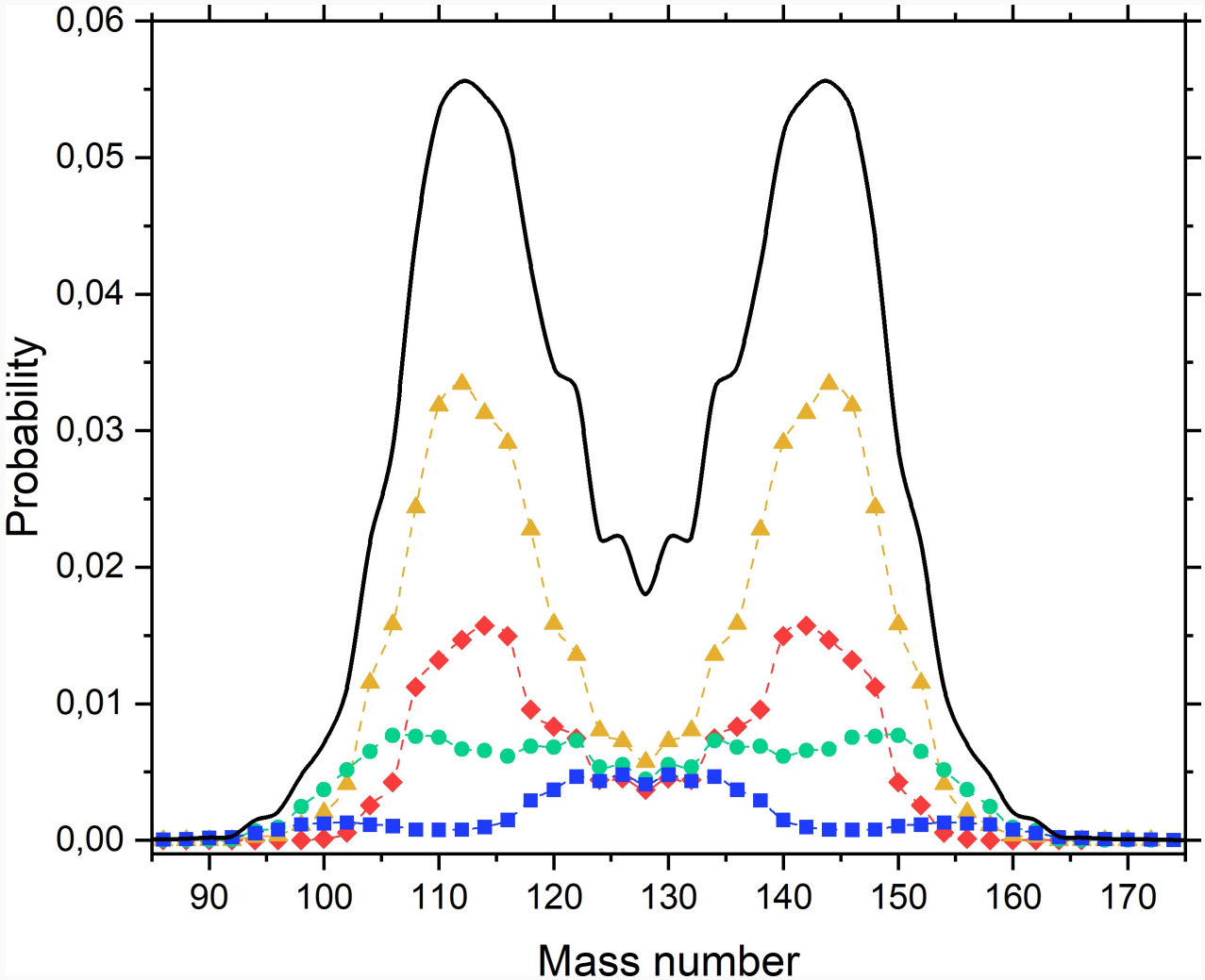

A.V. Isaev, et al., PLB **843**, 138008 (2023)

^{256}Rf: TKE distribution

solid line – overall;
squares: 0n – 1n;
circles: 2n – 3n;
triangles: 4n – 5n
rhombus: 6n – 9n.

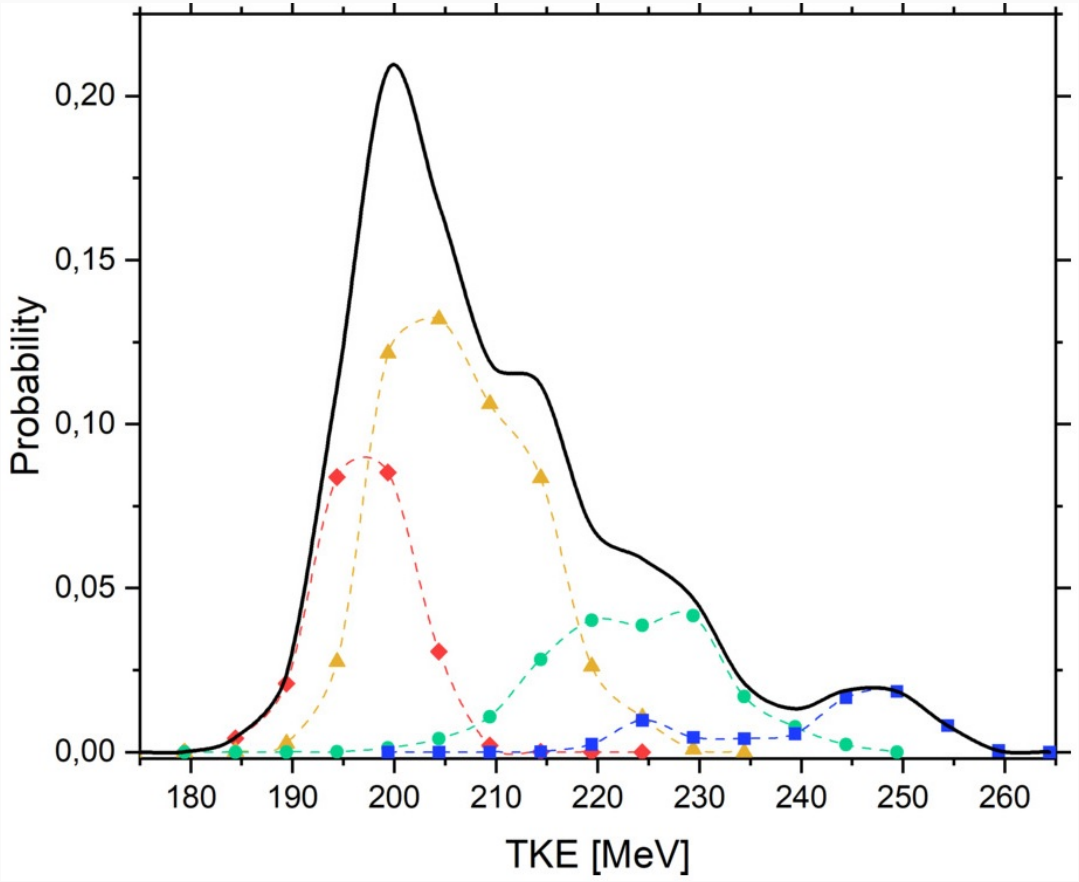

A.V. Isaev, et al., PLB **843**, 138008 (2023)

^{256}Rf: TKE distribution

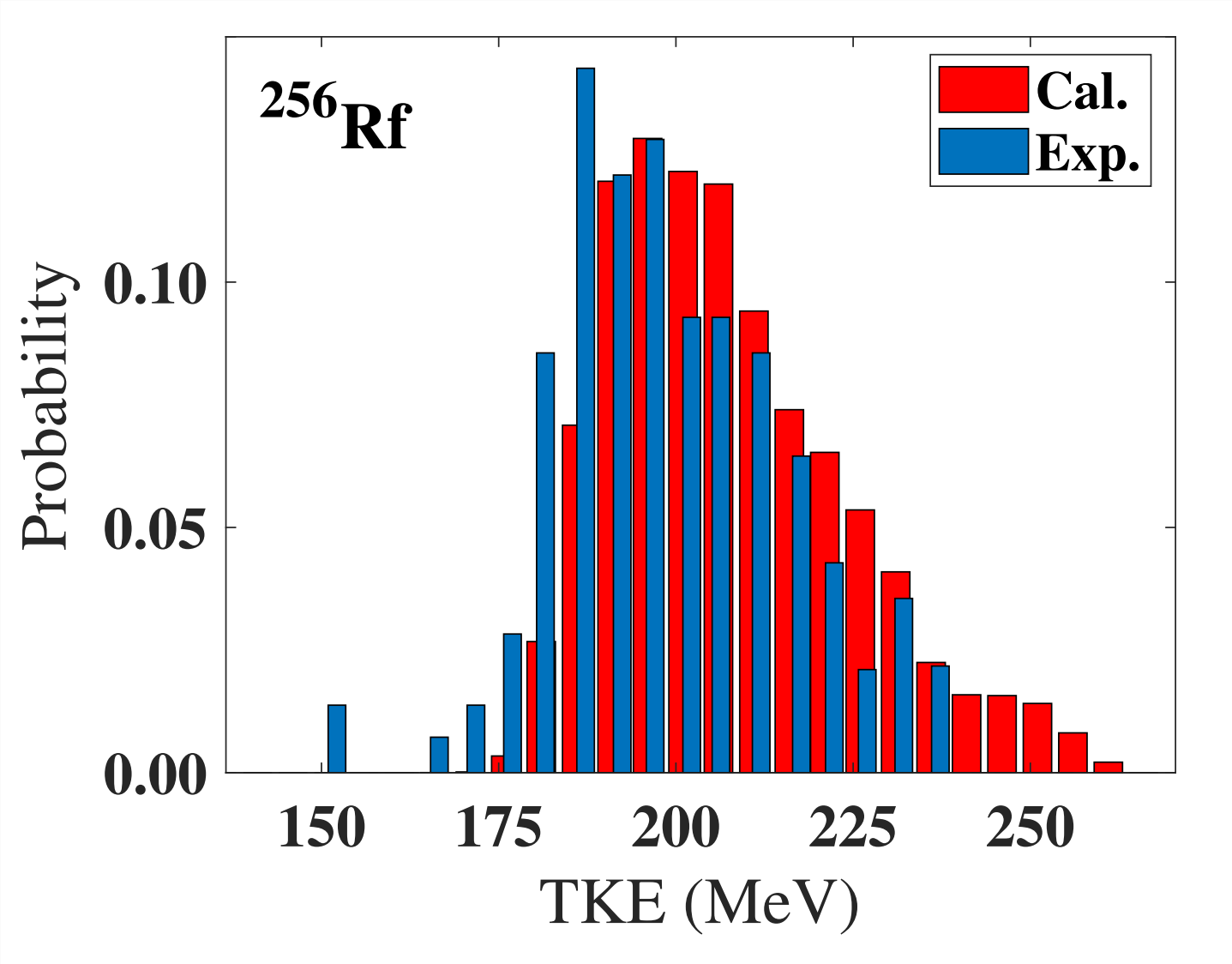

Exp. data from: P. Mosat, et al., Phys. Rev. C, **101**, 034310 (2020)

^{256}Rf: Evolution of DNS distribution

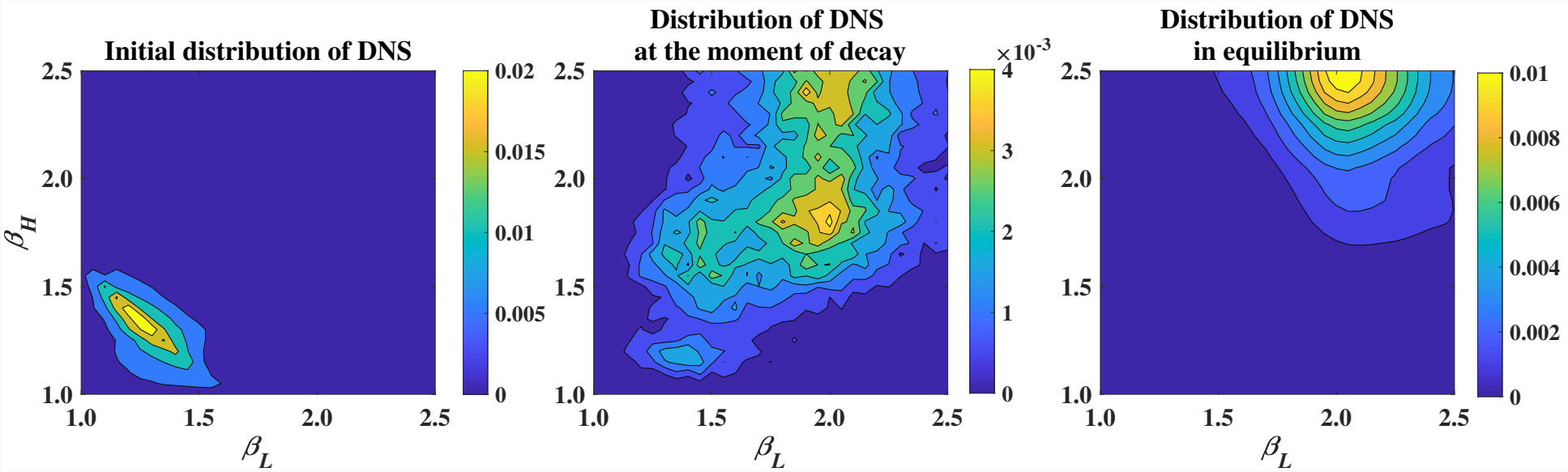

- Distribution of DNS at the moment of decay shows two wide maxima, one of which coincides with the maximum of the equilibrium distribution.
- Maximum corresponding to the compact shapes is mainly responsible for the emission of small number of neutrons.

^{256}Rf: Mass and charge distribution

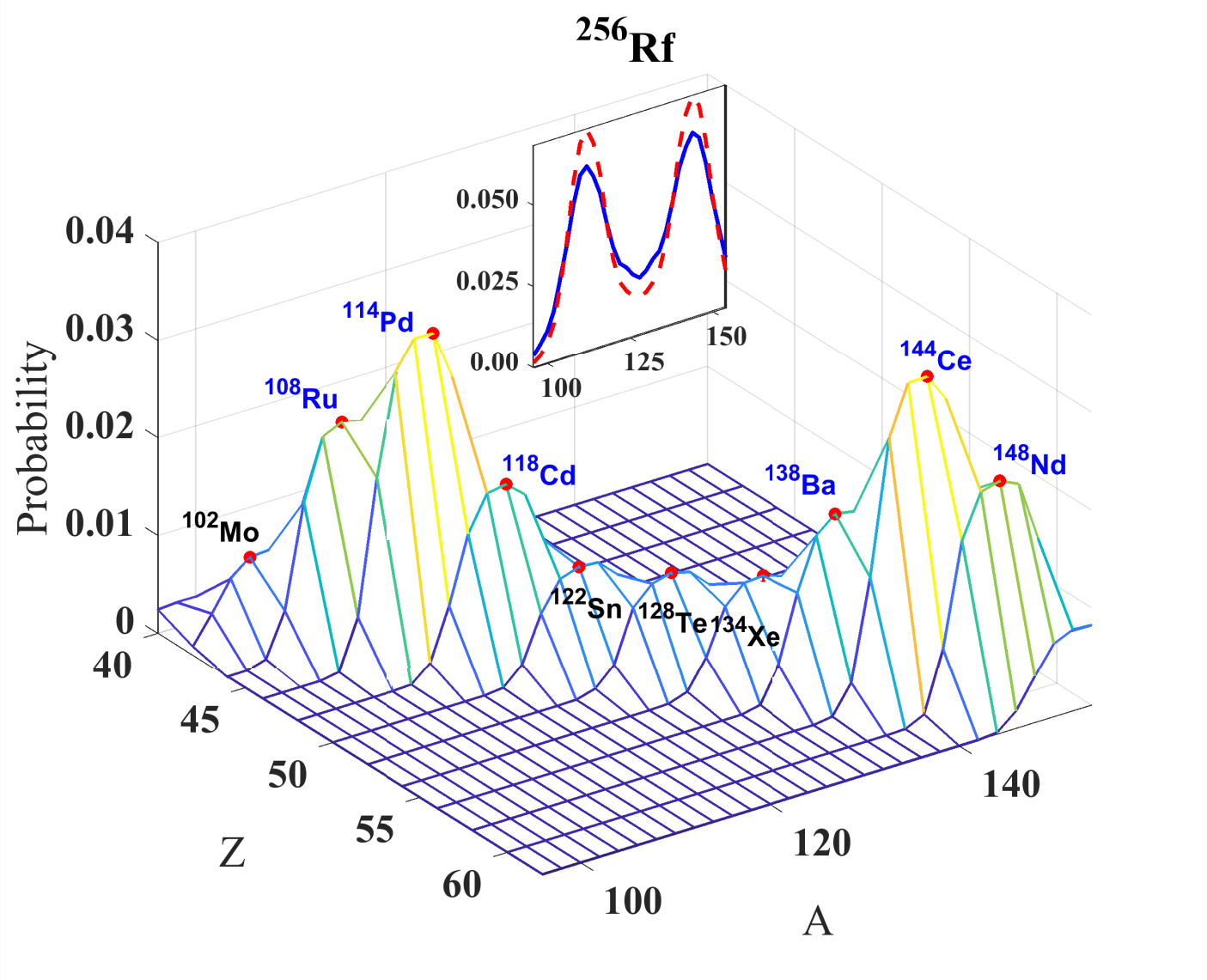

Inserted panel: red: eq. calc., blue: dyn. calc.

^{256}Rf: Potential energy of most probable DNS

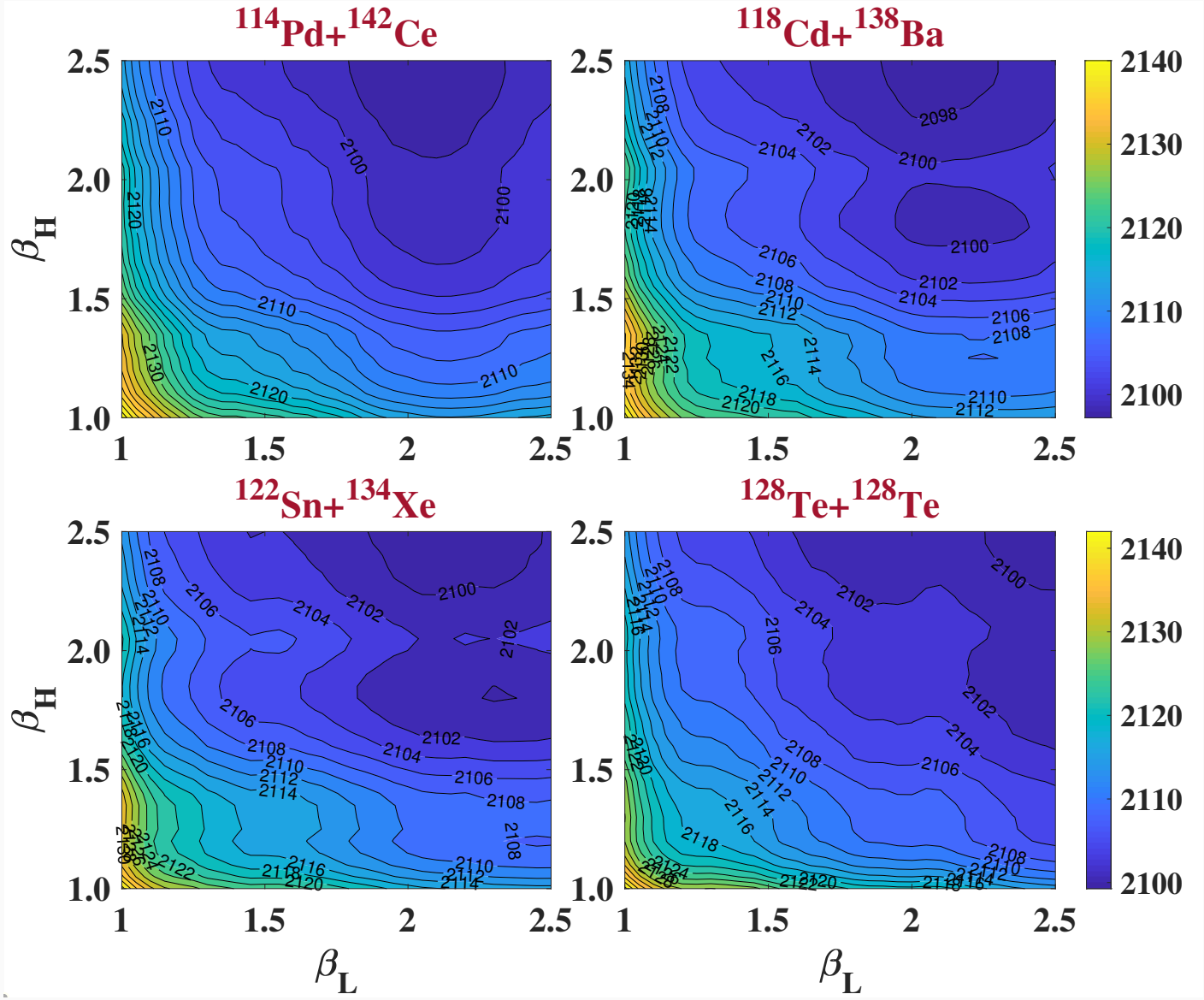

Neutron multiplicity: global fit

The parameters of the model were fixed by fitting the experimentally available data on neutron distribution for spontaneous fission of nuclei with $Z \sim 100$.

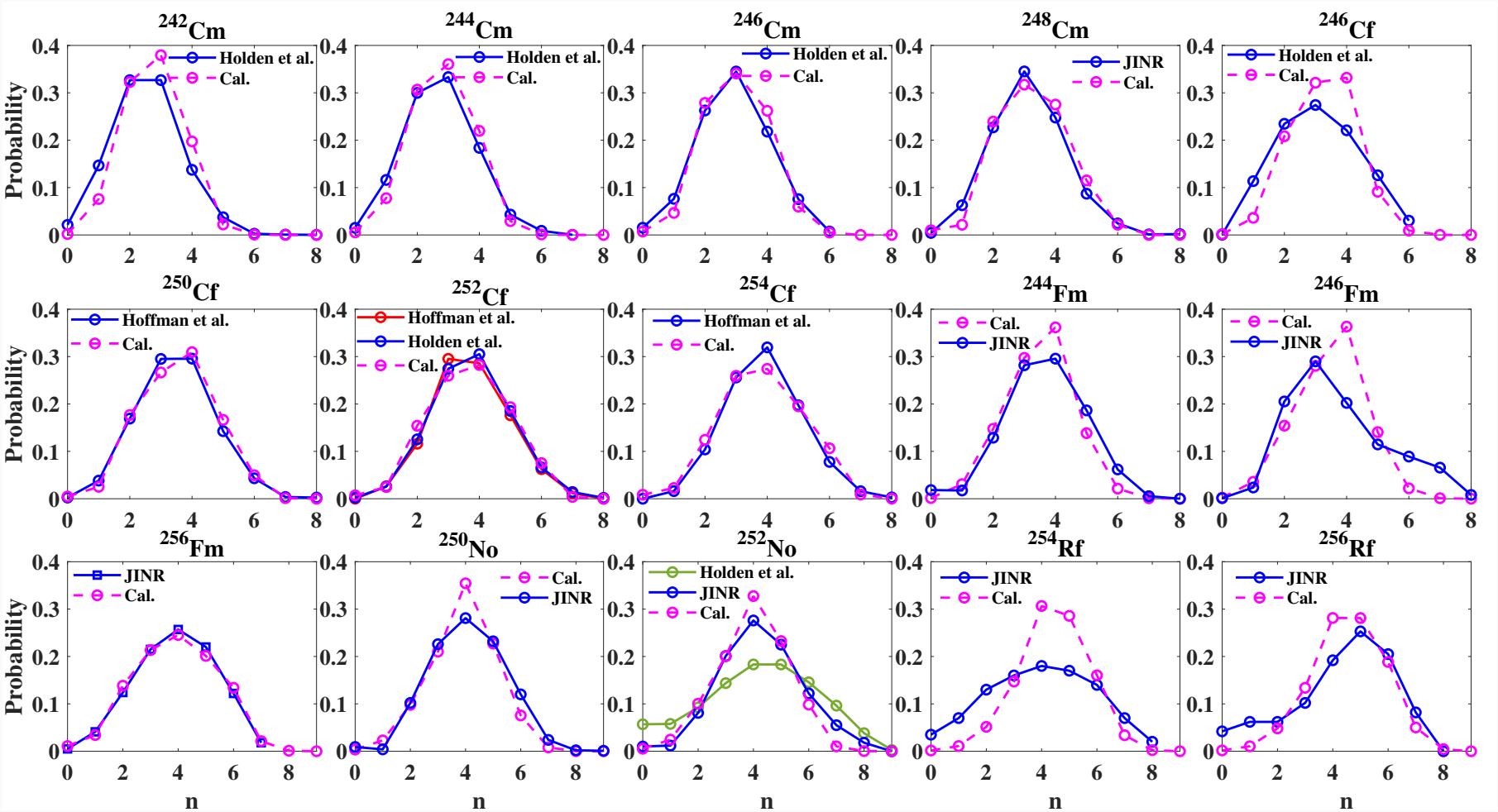

We obtain: $\lambda^{(A)} = 1.7$; $\lambda^{(\beta)} = 1.2$; $Q_{init} \sim 3.2 : 1$

Mass distributions of Fermium isotopes

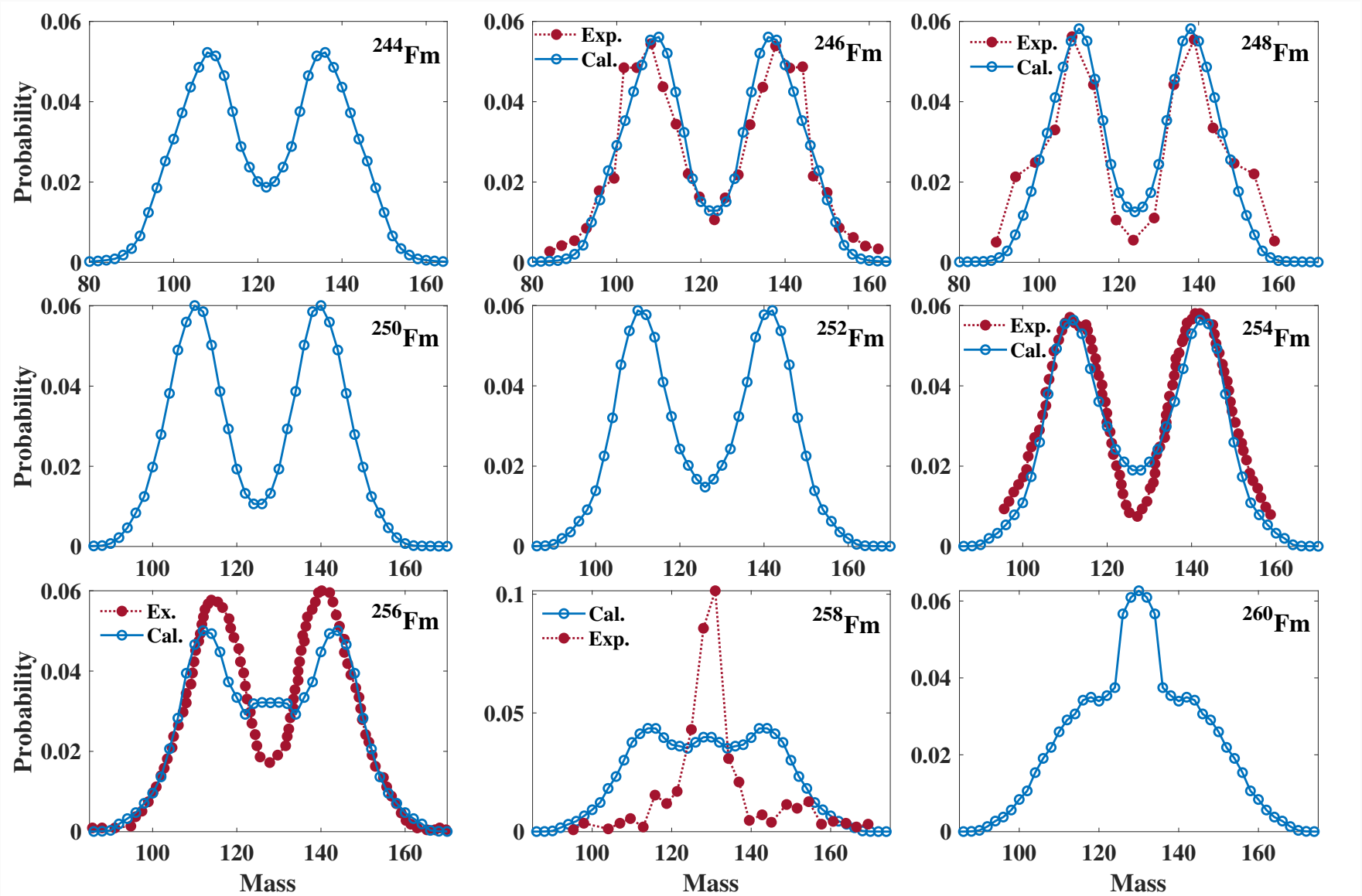

Thank You!